

Implications of headwater contact zones for the riverine barrier hypothesis: a case study of the Blue-capped Manakin (*Lepidothrix coronata*)

Andre E. Moncrieff¹, Brant C. Faircloth¹, Rosalind C. Remsen¹, Anna E. Hiller¹, Cristhian Felix², Angelo P. Capparella³, Alexandre Aleixo^{4,5,6}, Thomas Valqui^{2,7}, Robb T. Brumfield¹

¹Department of Biological Sciences and Museum of Natural Science, Louisiana State University, Baton Rouge, LA, USA

²Centro de Ornitología y Biodiversidad, Lima, Peru

³School of Biological Sciences, Illinois State University, Normal, IL, USA

⁴Programa de Pós-Graduação em Zoologia, Universidade Federal do Pará, Museu Paraense Emílio Goeldi, Belém, Brazil

⁵Finnish Museum of Natural History, University of Helsinki, Helsinki, Finland

⁶Instituto Tecnológico Vale—ITV, Belém, Brazil

⁷Facultad de Ciencias Forestales, Universidad Nacional Agraria La Molina, Lima, Peru

Corresponding author: Department of Biological Sciences and Museum of Natural Science, Louisiana State University, Baton Rouge, LA, 70803, USA.
Email: amoncr2@lsu.edu

Abstract

Rivers frequently delimit the geographic ranges of species in the Amazon Basin. These rivers also define the boundaries between genetic clusters within many species, yet river boundaries have been documented to break down in headwater regions where rivers are narrower. To explore the evolutionary implications of headwater contact zones in Amazonia, we examined genetic variation in the Blue-capped Manakin (*Lepidothrix coronata*), a species previously shown to contain several genetically and phenotypically distinct populations across the western Amazon Basin. We collected restriction site-associated DNA sequence data (RADcap) for 706 individuals and found that spatial patterns of genetic structure indicate several rivers, particularly the Amazon and Ucayali, are dispersal barriers for *L. coronata*. We also found evidence that genetic connectivity is elevated across several headwater regions, highlighting the importance of headwater gene flow for models of Amazonian diversification. The headwater region of the Ucayali River provided a notable exception to findings of headwater gene flow by harboring non-admixed populations of *L. coronata* on opposite sides of a < 1-km-wide river channel with a known dynamic history, suggesting that additional prezygotic barriers may be limiting gene flow in this region.

Keywords: Amazonia, contact zones, gene flow, headwaters, RADcap, rivers

Introduction

The Amazon Basin is one of the most species-rich areas on earth (Collen et al., 2014; Gentry, 1988; Jenkins et al., 2013; Valencia et al., 1994). This region's exceptional terrestrial biodiversity often conforms to a general biogeographic pattern: species distributions are delimited by the Amazon River and its major tributaries (Ayres & Clutton-Brock, 1992; Cracraft, 1985; Hayes & Sewlal, 2004; Sick, 1967; Wallace, 1852). Although barrier effects have been documented in many other river systems for a wide range of terrestrial taxa (Anthony et al., 2007; Brant & Ortí, 2003; Eriksson et al., 2004; Jackson & Austin, 2010; Jalil et al., 2008; Leaché & Reeder, 2002; Norris, 1958; Zhang et al., 2007), the extent and strength of this biogeographic pattern are pronounced in Amazonia. For this reason, Amazonia has been the focal region for a large body of research devoted to developing and testing what is known as the “riverine barrier hypothesis” (reviewed in Haffer, 1997; Leite & Rogers, 2013; Moritz et al., 2000), which generally states that rivers reduce migration

and promote allopatric speciation of opposite-bank populations (Capparella, 1987, 1988; Sick, 1967; Wallace, 1852).

The riverine barrier hypothesis has its origins in observations by Alfred Russel Wallace (Wallace, 1852), who noted that primate species were often limited to one side of major Amazonian rivers and acknowledged that “the native hunters are perfectly acquainted with this fact.” Additional studies in Amazonia have corroborated the idea that rivers commonly act as dispersal barriers in a diversity of taxonomic groups including plants (Nazareno et al., 2017, 2019), birds (Capparella, 1987; Cracraft, 1985; Hayes & Sewlal, 2004; Naka & Brumfield, 2018; Ribas et al., 2012), primates (Ayres & Clutton-Brock, 1992; Cortés-Ortiz et al., 2003), amphibians and squamates (Dias-Terceiro et al., 2015; Fouquet et al., 2015; Godinho & da Silva, 2018; Moraes et al., 2016; Souza et al., 2013), and butterflies (Hall & Harvey, 2002; Rosser et al., 2021). Allozyme variation in birds along the Napo and Amazon rivers further demonstrated that rivers delimit species ranges as well as the boundaries between intraspecific

Received May 15, 2023; revisions received October 6, 2023; accepted October 18, 2023

Associate Editor: Michael Whitlock; Handling Editor: Tim Connallon

© The Author(s) 2023. Published by Oxford University Press on behalf of The Society for the Study of Evolution (SSE). All rights reserved. For permissions, please e-mail: journals.permissions@oup.com

genetic clusters (Capparella, 1987, 1988). The presence of genetic structuring across Amazonian rivers has now been documented in numerous species (e.g., Aleixo, 2004; Armenta et al., 2005; Cortés-Ortiz et al., 2003; d'Horta et al., 2013; Fernandes et al., 2014; Naka & Brumfield, 2018; Nazareno et al., 2019), reinforcing the role of rivers as barriers to gene flow. This role can be played out in various scenarios including the division of continuous populations during river formation or rearrangement (Musher et al., 2022; Ribas et al., 2012, 2022) and the separation of populations established following dispersal across rivers (Brumfield, 2012; Smith et al., 2014).

One long-standing challenge to the idea that rivers create sufficient geographic isolation for allopatric speciation is that populations may come into contact along rivers as they narrow toward their headwaters (Haffer, 1992, 1997; Moritz et al., 2000). This river-narrowing is implicit in Wallace's (1852) observation that "on approaching the sources of the rivers they cease to be a boundary." A few studies have documented increased genetic similarity or hybridization between opposite-bank populations in headwater regions (e.g., Berv et al., 2021; Peres et al., 1996; Weir et al., 2015), supporting the idea that these regions may commonly hold contact zones. However, a fundamental limitation to understanding the role of headwater regions in permitting gene flow around river barriers is extremely sparse sampling, or the so-called "Wallacean shortfall" (Hortal et al., 2015; Lomolino, 2004), across these difficult-to-access regions (Oliveira et al., 2016; Oren & Albuquerque, 1991; Schulman et al., 2007). A second limitation is that studies of headwater contact zones have generally focused on a single region, preventing our understanding of whether different headwater regions show different patterns of genetic structure for widespread Amazonian taxa.

To test for genetic connectivity across Amazonian rivers toward their headwaters, we examine populations of the Blue-capped Manakin (*Lepidothrix coronata*), which is among the best-sampled Amazonian species in natural history collections. This species is found in the understory of *terra firme* forest and has been previously shown to contain several genetically and phenotypically distinct populations across the western Amazon Basin (Capparella, 1987; Cheviron et al., 2005; Moncrieff et al., 2022; Paulo et al., 2023; Reis et al., 2020). Previous work using allozymes (Capparella, 1987, 1988), mtDNA (Cheviron et al., 2005), and a combination of mtDNA and three nuclear loci (Paulo et al., 2023; Reis et al., 2020) showed that rivers including the Napo, Japurá, and, especially, the Amazon are genetic barriers for *L. coronata* populations. A phylogenetic study of the genus *Lepidothrix*, based on thousands of nuclear loci, supported two clades of *L. coronata* south of the Amazon on opposite sides of the Ucayali and a third clade north of the Japurá, but the relationships of individuals found between the Marañón/Amazon and Japurá rivers were unresolved (Moncrieff et al., 2022). In this same region of Amazonia, Berv et al. (2021) identified a lineage of White-crowned Manakins (*Pseudopipra pipra*) with mixed ancestry that suggested a history of genetic connectivity across the headwater region of the Amazon River in Peru.

Our current study seeks to identify patterns of headwater gene flow in *L. coronata* across the western Amazon Basin and to build on findings of headwater gene flow across individual rivers in the basin including the Amazon (Berv et al.,

2021), Juruá (Peres et al., 1996), and Tapajós rivers (Weir et al., 2015). These previous findings motivate our current study in which we use a well-sampled study species with a widespread distribution to simultaneously assess patterns of gene flow across multiple headwater regions of the Amazon drainage. We suspect the results of this study will be especially relevant for understanding genetic connectivity in Amazonian taxa restricted to *terra firme* or upland forests.

Bird communities of *terra firme* forest in Amazonia, which include *L. coronata* and over 1,000 other species of birds (Parker, 1996), experience a greater river barrier effect due to the additional effective river width provided by *várzea* or floodplain forests that flank rivers (Del-Rio et al., 2021; Remsen & Parker, 1983). Furthermore, bird species of dark, forest understory appear to show greater genetic divergence across rivers than canopy species (Burney & Brumfield, 2009), suggesting that species in different habitats have different dispersal capabilities or propensities. Dispersal-challenge experiments for another manakin species of forest understory, *Pipra filicauda*, resulted in mostly successful flights (36 out of 41) across distances of 100–400 m over open water, which suggests that the riverine barrier effect observed for *L. coronata* may be due more to its preference for the understory of *terra firme* forests rather than physical limitations in flight capability (Naka et al., 2022).

Given the life history traits and the wide geographic distribution and abundance of *L. coronata*, we consider this species well suited to assess the evolutionary implications of headwater contact zones in Amazonia and to test the hypothesis that gene flow across rivers increases toward their headwaters. Evidence for elevated gene flow toward river headwaters would highlight the breakdown in the barrier effect of rivers on approaching their sources and suggest that river barriers may be insufficient for the completion of the speciation cycle. If gene flow is not elevated toward river headwaters, one alternative is that gene flow across the middle and lower sections of rivers, perhaps facilitated by river course changes, is sufficiently high to produce similar levels of gene flow along the entire length of rivers. Another alternative is an absence of gene flow along the entire length of rivers, which would suggest that additional reproductive barriers between opposite-bank populations are preventing gene flow despite contact with populations in headwater areas. Throughout our study, we use the term "headwater region" to broadly refer to the narrower upper section (up to hundreds of km) of a river within the Amazonian lowlands (see Figure 1 in Haffer, 1992) and the terms "headwater contact zone" and "headwater gene flow" to refer to features of headwater regions rather than of the river source *sensu stricto*.

Methods

Sampling and DNA extraction

We extracted DNA from the tissues of 701 individuals and toepads of five individuals for a total of 706 *L. coronata* from 83 localities across its geographic range in the western Amazon Basin and eastern foothills of the Andes (Figure 1; Supplementary Table S1). Some of these 83 localities included several sublocalities within 10 km of each other that we merged for visualization purposes and for calculation of population differentiation (F_{ST} ; see Supplementary Table S1 for precise coordinates of all samples). We obtained samples from existing genetic resource collections at six different museums and fieldwork in Peru during 2018 and 2019 along

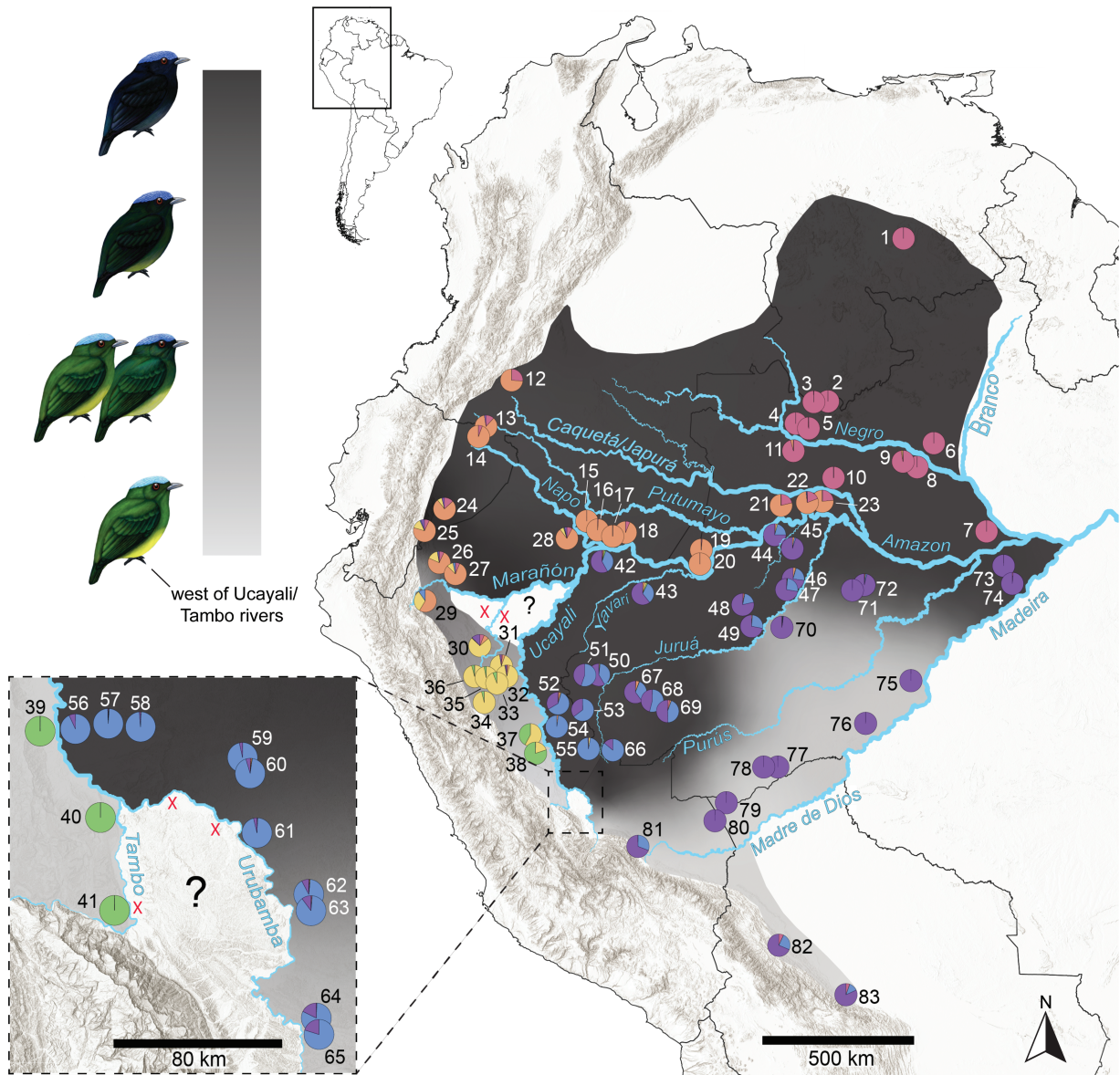


Figure 1. Map of *Lepidothrix coronata* genetic sampling localities across the western Amazon Basin with pie charts showing locality-averaged ancestry coefficients estimated by sNMF at the optimal $K = 6$ for dataset 4 (see [Supplementary Table S1](#) for complete sample information). The grayscale gradient and legend illustrate plumage color variation based on assessment of specimens, photographs from the Macaulay Library, and previous studies (Guilherme, 2016; Haffer, 1970; Moncrieff et al., 2022; Teófilo et al., 2018). The “X” marks indicate localities surveyed where we did not detect any individuals (Moncrieff et al., 2019, 2020), and question marks emphasize our uncertainty regarding the presence of *L. coronata* populations in the area.

the Ucayali, Urubamba, and Tambo rivers (Moncrieff et al., 2020; see Acknowledgments for museum sources and permit information). Tissues consisted of pectoral muscle preserved in liquid nitrogen or ~95% ethanol. We used DNeasy Blood & Tissue Kits (Qiagen, Hilden, Germany) to extract total DNA for all tissues, and we assessed extract quality using gel electrophoresis. We found that eight tissues had especially short DNA fragments, indicating DNA degradation (see [Supplementary Table S1](#)). To extract DNA from toepads, we used a phenol-chloroform protocol (Tsai et al., 2020), and we quantified all extracts using a Qubit 2.0 Fluorometer (Life Technologies, Carlsbad, California, USA).

DNA probe design, library preparation, enrichments, and sequencing

To collect reduced representation SNP data from all samples, including toepads, we used RADcap (Hoffberg et al., 2016),

as previously described (Moncrieff et al., 2022). In brief, we designed custom sequence capture baits using a pilot RADseq dataset and the reference *L. coronata*-1.0 genome (NCBI RefSeq assembly accession GCF_001604755.1; scaffold N50: 5.0 Mb; scaffold L50: 70) that targeted 2,495 variable loci from putatively non-coding regions separated by > 75 kb on reference genome scaffolds > 1 Mb. Then, we prepared genomic libraries from tissues using dual-digest RADseq (3RAD; Bayona-Vásquez et al., 2019), except for eight degraded tissue samples (see [Supplementary Table S1](#)). We prepared standard genomic libraries for the eight degraded tissue samples and five toepad samples using a KAPA HyperPrep library preparation kit (F. Hoffmann-La Roche AG, Basel, Switzerland) and iTru indexes (Glenn et al., 2019). We combined libraries at equimolar ratios into pools of eight, and we enriched RAD loci from each pool using the custom sequence capture baits targeting RAD loci and following the manufacturer’s protocol

Table 1. Summary of SNP datasets used in this study.

Dataset	Individuals	Minimum site completeness	Minor allele frequency cutoff	SNPs	Mean depth/SNP (range of means)	Mean missingness/SNP
1	706	75%	5%	1595	28–120	2.1%
2	706	95%	5%	1408	41–167	0.8%
3	387	75%	5%	1663	29–114	2.4%
4	387	95%	5%	1436	42–161	1.0%
5	14	100%	None	1939	35–191	0%
6	20	100%	None	1955	36–149	0%
7	20	100%	None	1773	32–143	0%

v4.01 (myBaits Custom Kit; Daicel Arbor Biosciences, Ann Arbor, Michigan, USA). Prior to sequencing, we combined enrichment pools at equimolar ratios, except for pools of degraded samples for which we added an additional 25% volume. We sequenced samples across parts of three lanes of paired-end, 150 base-pair sequencing on an Illumina HiSeq X (Novogene Corporation Inc., Sacramento, CA, USA).

Initial DNA sequence data processing

We initially processed sequence data as described by Moncrieff et al. (2022). In summary, we received FASTQ files from the sequencing center, demultiplexed reads using BMap (Bushnell, 2014) and Stacks (Catchen et al., 2013), and aligned sequence data to the *L. coronata* reference genome using BWA (Li & Durbin, 2009) and SAMtools (Li et al., 2009) to produce BAM files. Next, we conducted one round of base quality score recalibration (BQSR) on each lane of samples using GATK *BaseRecalibrator* and *ApplyBQSR* (Van der Auwera & O'Connor, 2020). Using the recalibrated BAM files, we jointly called variants for all individuals using GATK *HaplotypeCaller*, *GenomicsDBImport*, and *GenotypeGVCFs*, and we used VCFtools 0.1.16 (Danecek et al., 2011) to quality filter the results by removing variants outside the 2,495 targeted loci, individuals with mean depth < 10× across targeted loci, low-quality sites (--minQ 30), indels (--remove-indels), and non-biallelic sites (--min-alleles 2 --max-alleles 2), resulting in a “clean” Variant Call Format (VCF) file.

SNP datasets

Because we were interested in examining the effects of data filtering on our results, we prepared several SNP datasets using different samples and levels of site filtering. We began by creating two VCF files representing different sampling schemes of individuals: (a) a file containing all individuals in the dataset (identical to the “clean” VCF file that resulted from our initial processing in the previous section) and (b) a file containing a maximum of 10 individuals per locality (for localities with > 10 individuals, we retained individuals with the least missing data; many localities had fewer than 10 individuals). Once we prepared these files with different samples of individuals, we used VCFtools to ensure the included sites had a depth of ≥ 15× (--minDP 15) and a minor allele frequency ≥ 0.05 (--maf 0.05). To examine the effects of site completeness, we created two files for each sample of individuals having ≥ 75% and ≥ 95% site completeness (--max-missing 0.75; --max-missing 0.95). Lastly, we thinned each of these four VCF files by removing sites < 75 kb apart (--thin 75000; equivalent to retaining no more than one SNP per RADcap locus; datasets 1–4 in Table 1).

To test demographic models for different opposite-bank locality pairs, we created three additional VCF files from the “clean” VCF file that resulted from our initial processing. We first subset the “clean” VCF file to create three VCF files with different sets of individuals from specific locality pairs (see Figure 1 and Supplementary Table S1): 21 and 44 (dataset 5), 17 and 42 (dataset 6), and 15 and 28 (dataset 7), retaining a maximum of 10 individuals per locality (as described above). We further removed all sites with missing data (--max-missing 1), sites with < 15× depth (--minDP 15), invariant sites created by subsetting (--mac 1), and sites < 75 kb apart (--thin 75000). We then used VCFtools to calculate the mean depth and missingness for each SNP for all datasets (Table 1; Supplementary Tables S2–S8).

Genetic structure and gene flow

To examine how rivers structure *L. coronata* populations across the western Amazon Basin, we estimated ancestry coefficients for datasets 1–4 assuming different numbers of ancestral populations using the sNMF function (Frichot et al., 2014) implemented in R package LEA 3.6.0 (Frichot & François, 2015). We set $K = 10$ as the upper bound for the number of ancestral populations after test runs showed that cross-entropy was consistently lower with fewer than 10 populations. We conducted analyses for each dataset that consisted of 100 replicate runs of ancestry coefficient estimation at 10 values of K (1–10) across four values of the alpha regularization parameter (1, 10, 100, and 1,000). For each dataset, we identified the alpha regularization parameter value that consistently provided the lowest mean cross-entropy values at different values of K (Supplementary Tables S9–S12), and we input the associated set of sNMF runs ($K = 2–10$) into the online version of CLUMPAK (Kopelman et al., 2015; accessed March 2022) to summarize replicate runs and visualize ancestry coefficients (Supplementary Figures S1–S4). Because visualizing genetic variation in a geographic context across multiple datasets at multiple K values is difficult, we also identified the value of K that best fit each dataset by selecting the value after which cross-entropy values decreased slightly (by < 0.001) for successive values of K (Supplementary Tables S9–S12). Then, we compared cross-entropy values of replicates at these “best” K values across datasets and identified dataset 4 as having the replicate with the lowest cross-entropy (at $K = 6$; Supplementary Table S12). Using this sNMF replicate (from dataset 4, $K = 6$), we averaged the ancestry coefficients across individuals at each locality and used QGIS 3.20 (QGIS, 2021) to map average ancestry coefficients to localities (Figure 1). Due to dataset 4 having slightly lower cross-entropy values across K s in sNMF analyses, a maximum of 10 individuals

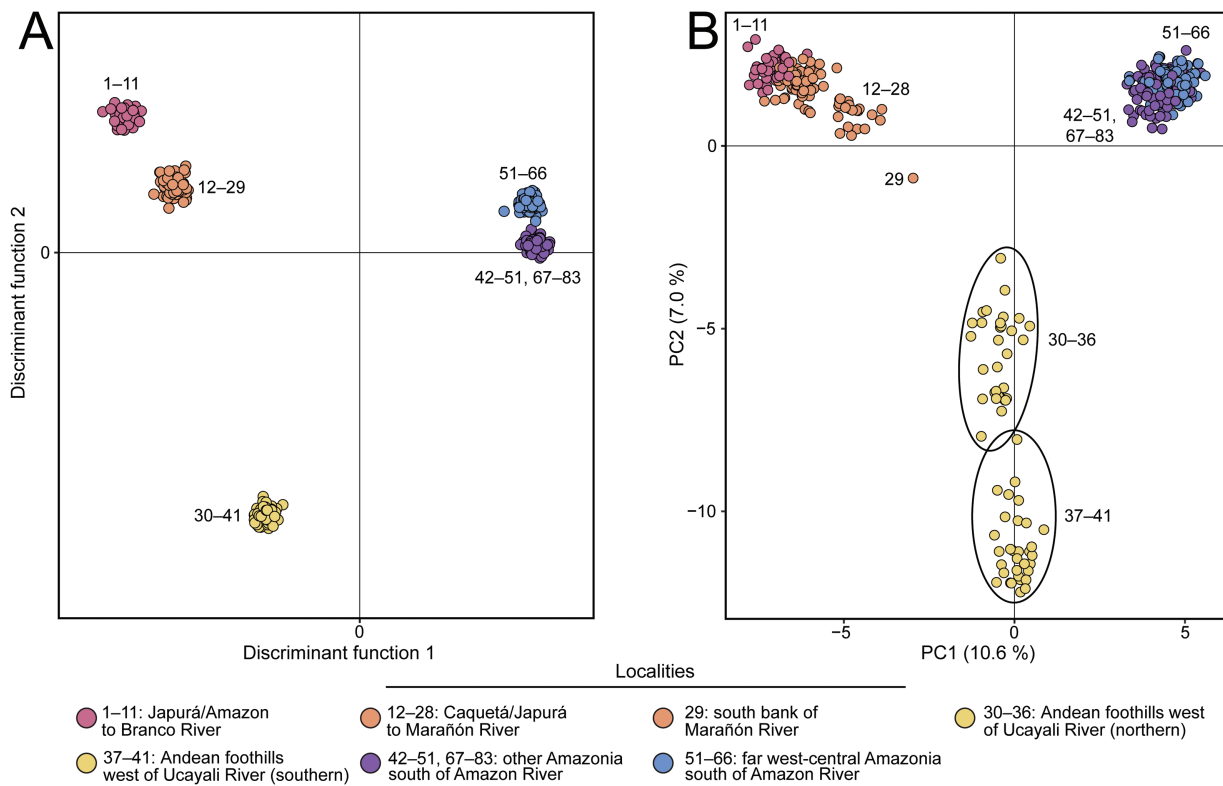


Figure 2. (A) Discriminant analysis of principal components of dataset 4 with the first two discriminant functions showing relatedness among genetic clusters of *Lepidothrix coronata* at $K = 5$, which was the optimal value inferred after K -means clustering and minimizing the Bayesian information criterion (BIC; see *Methods*). (B) Principal component analysis of dataset 4 showing the first two axes (PC1 and PC2) and percent genetic variance explained, with individuals colored by population assignments from K -means clustering. Locality numbers refer to those in Figure 1 and Supplementary Table S1. Note that locality 51 contains individuals assigned to different populations (Supplementary Table S16).

per locality (providing more even sampling and reduced computation time for subsequent analyses, particularly EEMS), and minimal missing data, we selected this dataset for several analyses described below.

Because we were interested in visualizing patterns of relatedness between genetic clusters, we conducted a discriminant analysis of principal components (DAPC) for datasets 1–4 (Jombart et al., 2010). We used the K -means *find.clusters* function in Adegenet 2.1.5 (Jombart & Ahmed, 2011) run in R version 4.1.1 (R Core Team, 2021) to estimate the optimal number of populations (K), retaining all principal components and increasing K until the slope in plots of K versus the Bayesian information criterion (BIC) decreased only slightly, as if approaching an asymptote, or began to increase (Supplementary Figures S5–S8). Then, we used the *dapc* function to calculate maximal differences among populations, retaining 450 (datasets 1 and 2) or 300 (datasets 3 and 4) principal components and all four discriminant functions (Figure 2A; Supplementary Figures S9–S12). Finally, to investigate the major axes of genetic variation across all individuals, we conducted a principal components analysis (PCA) in Adegenet 2.1.5 (Jombart & Ahmed, 2011) for datasets 1–4 using the *dudi.pca* function (Figure 2B; Supplementary Figures S13–S16), and we colored individuals according to their population assignments inferred by K -means clustering (Supplementary Tables S13–S16).

To investigate whether river barriers have caused populations across the landscape to deviate from an isolation-by-distance model and to estimate geographic areas of higher- or lower-than-average gene flow, we calculated an estimated

effective migration surface using the EEMS pipeline (GitHub commit c1849ea; Petkova et al., 2016). We computed a full-rank Euclidean distance matrix of average pairwise genetic distances between all 387 individuals using dataset 4 and the *strdiffs* pipeline, and we selected the *Diff_s_v1* output since our data met the necessary requirements (Petkova, 2016). Then, we prepared files of (a) individual coordinates and (b) coordinates defining the polygon within which we wanted to estimate the migration surface (the approximate geographic distribution of *L. coronata*). Next, we performed several test runs (*runeems_snps*) using random seeds and spatial grids of up to 1 K demes (georeferenced individuals associated with the nearest deme) to tune the migration (*mEffctProposalS2*, *mSeedsProposalS2*, and *mrRateMuProposalS2*) and diversity (*qEffctProposalS2*, *qSeedsProposalS2*) proposal variances and achieve an acceptance rate of 20%–30%, improving sampling of parameter space (Petkova, 2017). After parameter tuning, we ran three independent Markov chain Monte Carlo (MCMC) chains with *runeems_snps* using random seeds, a spatial grid of 1 K demes, and 4 M iterations of MCMC. We discarded the first 2 M iterations as burn-in, sampled the posterior distribution every 10 K iterations, and evaluated posterior traces produced by *eems.plots* to ensure adequate convergence of the three MCMC chains by looking for similar values, horizontal trajectories, and overlapping amplitudes (Petkova, 2017). We used the R package *rEEMSplots* to prepare a map overlaid with a continuous estimated effective migration surface (Figure 3A) and a map highlighting regions where the posterior probabilities were above 90% for an estimated migration rate (m) above or below the mean (Figure 3B).

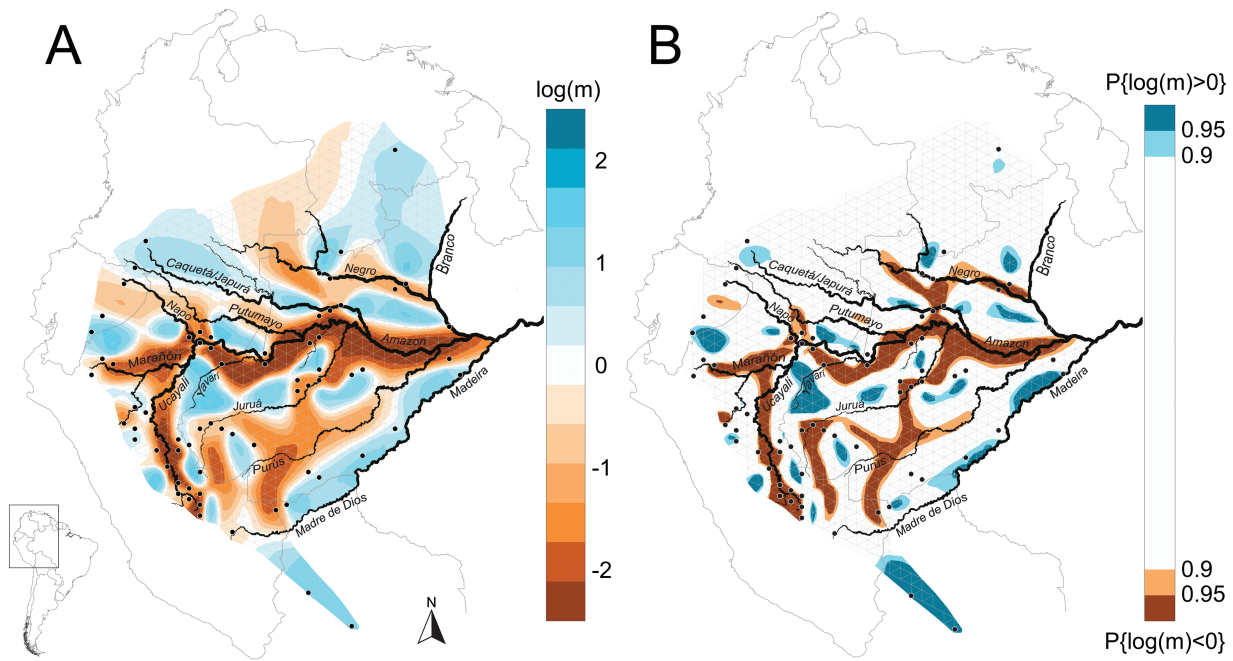


Figure 3. (A) Effective migration rate (m), a proxy for gene flow calculated using EEMS, across the western Amazon Basin based on a genetic distance matrix of 387 georeferenced individuals of *Lepidothrix coronata* (dataset 4). The \log_{10} scale for effective migration is normalized so that 0 is the mean migration rate under an isolation by distance model, negative values (browns) indicate lower migration than expected, and positive values (blues) indicate higher migration than expected. (B) Posterior probabilities of effective migration rate (m) estimates presented in (A). This map illustrates the most likely corridors for gene flow by highlighting areas in blue where posterior probabilities $p\{\log(m) > 0\}$ exceed 90% while simultaneously emphasizing the most likely barriers for gene flow by highlighting areas in brown where posterior probabilities $p\{\log(m) < 0\}$ exceed 90%. Points shown in (A) and (B) are not exact localities of individuals; rather, they represent the localities shifted to the nearest vertex on the population grid ($n\text{Demes} = 1,000$), as required for the calculation of the effective migration surface.

Relationships of riverine variables to population differentiation

One challenge to the riverine barrier hypothesis is the idea that opposite-bank populations may come into contact with river headwaters, so we wanted to examine more directly the relationships of river width, floodplain width, and distance from river source to population differentiation between opposite-bank populations. We first identified opposite-bank localities along the Amazon and its 10 largest tributaries based on annual discharge (Gibbs, 1967). To select opposite-bank locality pairs, we limited each locality to a single comparison per river with the nearest (< 150 km) opposite-bank locality with no obvious additional geographic barriers intersecting the straight line between them. We retained only those locality pairs with a minimum of two individuals at each locality. This locality selection scheme resulted in eight opposite-bank locality pairs along the Amazon and five of its largest tributaries (Supplementary Table S17). One locality (locality 44 in Figure 1) was involved in two comparisons involving distinct rivers: cross-Amazon (localities 21–44) and cross-Jutaí (localities 44–45). Using Google Earth Pro v7.3 to access Landsat/Copernicus satellite imagery from December 2020, we drew straight lines between opposite-bank localities and measured a representative width of the main river channel where the straight line bisected the river or at a location that was slightly shifted to avoid measurements where the presence of river islands exaggerated river widths (Supplementary Figure S17). We also measured the straight-line distance between the nearest opposite-bank “non-wetland” areas in the vicinity of our sampled localities, ensuring that the straight line between

“non-wetland” areas intersected over the river with the straight line between opposite-bank localities; the “non-wetland” areas were based on the Amazonian wetland extent, cover, and flooding layer generated by Hess et al. (2015). Hereafter, we refer to this distance as the floodplain width. Finally, we measured the distance of opposite-bank localities from the source of the river using 10-km increments to follow the river course until reaching the straight line between opposite-bank localities (Supplementary Table S17). Next, we used VCFtools to compute Weir and Cockerham’s weighted F_{ST} between paired localities based on dataset 4. Because we predicted that population differentiation would increase with greater river width, floodplain width, and distance from river source, we computed one-sided Spearman’s rank-order correlations in R with the base *cor.test* function between population differentiation (F_{ST}) of opposite-bank populations and: (a) river width, (b) floodplain width, and (c) distance from river source (Figure 4; Supplementary Table S17). We performed these three correlation analyses again (Supplementary Figure S18) after removing a single-locality pair across the upper Ucayali River due to the different landscape features across the river, which potentially made the locality pair unsuitable for measuring a river barrier effect. Specifically, the cross-Ucayali locality pair included population 39 which was in Andean foothills and population 56 which was in Amazonian lowlands (inset, Figure 1); all other locality pairs occupied lowland forest on both riverbanks. Other variability in habitat, fluvial geomorphology, elevation, and location of river source likely influences the strength of river barriers and is not accounted for by the three river metrics we used in these correlation analyses.

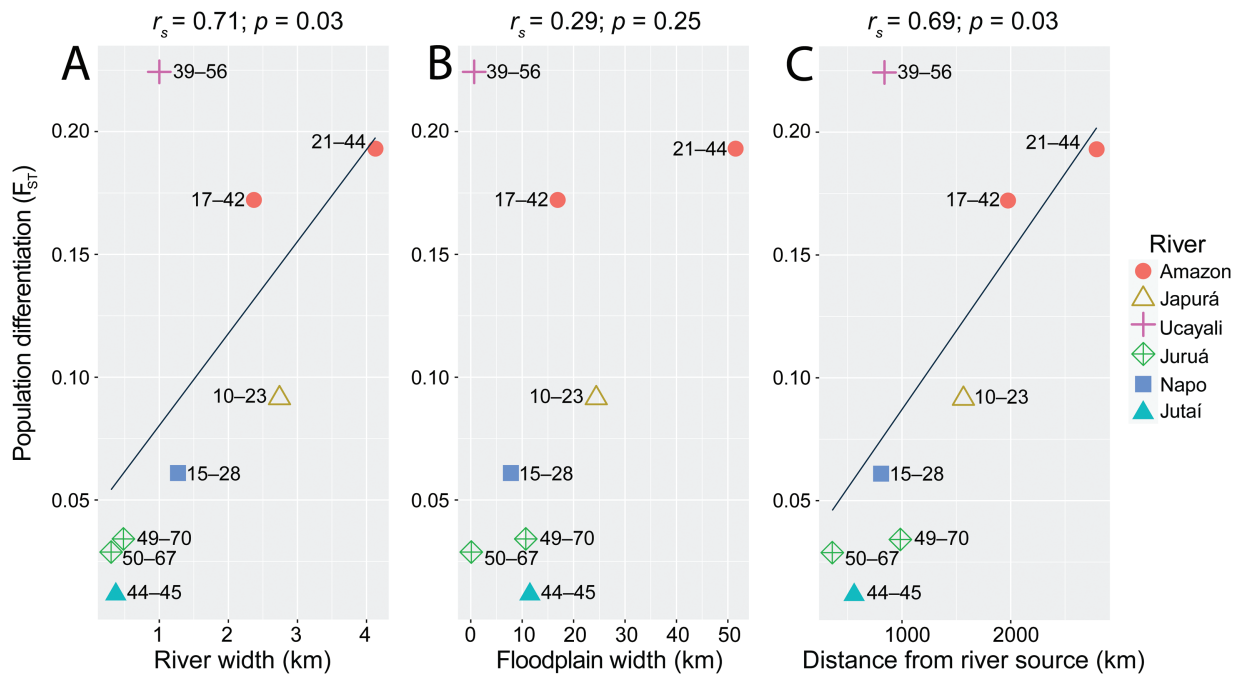


Figure 4. Scatterplots of values for population differentiation (F_{ST}) between opposite-bank populations of *Lepidothrix coronata* along major rivers of the western Amazon Basin and (A) river width, (B) floodplain width, and (C) distance from river source. Correlation coefficients and p -values for one-tailed Spearman's rank-order correlations shown above each panel. The paired numbers next to each plotted shape refer to locality numbers in Figure 1 and Supplementary Table S1.

Demographic analyses

To further test the hypothesis that gene flow across rivers increases toward their headwaters, we evaluated competing demographic models for populations along different sections of the Amazon drainage. First, we selected the three best-sampled cross-river locality pairs (the only such pairs with at least four individuals per locality), which were located at strategic points for comparisons along the Amazon drainage: (a) populations 21 and 44 across the upper Amazon River (dataset 5; 2,790 km from river source; see Figure 1, Table 1, and Supplementary Table S1); (b) populations 17 and 42 across the far upper Amazon River (dataset 6; 1,975 km from river source); and (c) populations 15 and 28 across the lower Napo River (dataset 7; 808 km from river source). For each of these three locality pairs, we evaluated four demographic models using momi v2.1.20 (Kamm et al., 2020): no migration, low migration, medium migration, and high migration (Supplementary Figure S19). As input to momi, we provided an ancestral effective population size of 500 K, which is comparable to previous estimates for other widespread Amazonian suboscines (Luna et al., 2022; Thom et al., 2020). We also ran momi analyses with ancestral population sizes of 100 K and 2 M (Supplementary Tables S18 and S19) to assess the sensitivity of our models to this parameter; however, model likelihoods were extremely similar (identical to four decimal places) to those estimated from models with ancestral population size inputs of 500 K (Table 2; Supplementary Table S20), so we do not report further on these additional model runs. We used two additional inputs for demographic models: (a) a generation time of 2 years based on the age when individuals of *L. coronata* acquire definitive plumage and presumably reach sexual maturity (1 year; Scholer et al., 2022) multiplied by two, which approximates the average age of females producing a clutch (see Nadachowska-Brzyska et al., 2015), and

(b) a germline mutation rate of 4.6×10^{-9} mutations per site per (2-year) generation estimated for another passerine bird, *Ficedula albicollis* (Smeds et al., 2016). We designed models to include: (a) a parameter for time of population divergence within the last 4 Myr, an upper bound that contains all previous divergence time estimates for *L. coronata* populations across the Amazon and Napo rivers (Cheviron et al., 2005; Paulo et al., 2023; Reis et al., 2020), (b) parameters for the size of each population, and (c) parameters for time of migration for the three models including this event. Specifically, each migration model included three bidirectional pulses of migration (after population divergence) occurring at different rates depending on the model: 1% (low migration model), 5% (medium migration model), or 10% (high migration model) of the populations. We considered it reasonable to include three pulses of migration in each model given the frequency and size of river captures transferring *terra firme* forest across rivers in the Amazon drainage over the last 100 kyr (Ruokolainen et al., 2019), and we allowed momi to optimize the timing of these pulses in each model. We used the momi functions *read_vcf* and *extract_sfs* to generate a site-frequency spectrum for each dataset and the *optimize* function to calculate model likelihoods and parameter estimates. We ran each model 100 times and selected the run with the highest likelihood. To identify the best models, we used the highest likelihood for each model to calculate the Akaike information criterion (AIC) and Akaike weights (Akaike, 1974; Burnham & Anderson, 2002). We also calculated two versions of the corrected AIC, AIC_c , and associated Akaike weights (Burnham & Anderson, 2002; Hurvich & Tsai, 1989), trying both $n =$ number of individuals and $n =$ number of SNPs in the AIC_c formula, since the interpretation of what constitutes the most natural unit for sample size in model testing varies across studies (e.g., O'Meara et al., 2006; Posada & Crandall, 2001; Salter et al., 2023).

Table 2. Summary of results from demographic analyses conducted in the program momi.

Populations	Distance from river source (km)	Model	K	Max. ln(L)	AIC	AIC _c (n = no. of SNPs)	AIC _c (n = no. of indiv.)	w _i (AIC)	w _i (AIC _c) (n = no. of SNPs)	w _i (AIC _c) (n = no. of indiv.)
21 and 44 ^a	2790	No mig.^b	3	-5,399.43	10,804.85	10,804.86	10,807.25	0.87	0.87	1.00
		Low mig.	6	-5,399.43	10,810.85	10,810.89	10,822.85	0.04	0.04	0.00
		Med. mig.	6	-5,399.43	10,810.85	10,810.89	10,822.85	0.04	0.04	0.00
		High mig.	6	-5,399.43	10,810.85	10,810.89	10,822.85	0.04	0.04	0.00
17 and 42	1975	No mig.	3	-5,901.97	11,809.93	11,809.95	11,811.43	0.19	0.19	0.74
		Low mig.	6	-5,897.62	11,807.23	11,807.28	11,813.70	0.74	0.74	0.24
		Med. mig.	6	-5,900.14	11,812.27	11,812.31	11,818.73	0.06	0.06	0.02
		High mig.	6	-5,901.97	11,815.93	11,815.98	11,822.40	0.01	0.01	0.00
15 and 28	808	No mig.	3	-5,343.27	10,692.53	10,692.55	10,694.03	0.00	0.00	0.00
		Low mig.	6	-5,324.32	10,660.64	10,660.69	10,667.10	0.00	0.00	0.00
		Med. mig.	6	-5,307.25	10,626.51	10,626.55	10,632.97	0.82	0.82	0.82
		High mig.	6	-5,308.78	10,629.55	10,629.60	10,636.01	0.18	0.18	0.18

Note. K = number of model parameters; Max. ln(L) = maximum log-likelihood; AIC = Akaike information criterion; AIC_c = corrected AIC; w_i = Akaike weight.

^aPopulation numbers refer to localities numbered in Figure 1 and Supplementary Table S1.

^bModels with highest support for each population pair according to Akaike weights in bold.

Results

DNA sequencing

Illumina sequencing produced an average of 1.4 M read pairs/sample (range 100 K–3.9 M) for the 693 non-degraded tissue samples, 5.4 M read pairs/sample (range 3.0–9.3 M) for the eight degraded tissue samples, and 10 M read pairs/sample for the five toepads (range 5.0–23.2 M; Supplementary Table S1). After removing PCR duplicates and off-target reads (those not overlapping any of the 2,495 RADcap loci), we retained averages of 628 K read pairs/sample (range 46 K–2.0 M) for non-degraded tissues, 127 K read pairs/sample (range 47–284 K) for degraded tissue samples, and 230 K read pairs/sample (range 65–489 K) for toepads (Supplementary Table S1). Across all datasets, mean depth per SNP ranged from 28 to 191; mean missingness per SNP for datasets 1–4 ranged from 0.8%–2.4% (Table 1; Supplementary Tables S2–S8).

Genetic structure and gene flow

sNMF ancestry coefficient estimates for *L. coronata* across the western Amazon Basin were consistent across datasets 1–4 (Figure 1; Supplementary Figures S1–S4), and we observed support for optimal Ks of 6 and 7 based on cross-entropy values (Supplementary Tables S9–S12). Examining ancestry coefficients from a range of K values (Supplementary Figures S1–S4) helped explain the hierarchy of genetic structure across the landscape. At K = 2 and K = 3, the Amazon and Ucayali rivers, respectively, consistently divided populations—highlighting their role as the barriers between the deepest genetic breaks within *L. coronata*; at higher K values, rivers such as the Japurá and Napo further subdivided more closely related populations. Generally speaking, populations occupied entire interflaves, although at higher K values, some individuals were assigned to populations located in areas without apparent geographic barriers such as the population east of the upper Ucayali River (blue in Figure 1), which consistently appeared at K ≥ 5 in all sNMF analyses. Ancestry coefficients were similar across the Yavarí, Juruá, and Purús rivers, which

is consistent with previous findings showing that relatively few taxa are separated by these rivers (Gascon et al., 2000; Haffer, 1997; Johnson et al., 2021; Lane et al., 2003; Rego et al., 2023; but see Del-Rio et al., 2021). This finding is possibly related to the dynamic history of these particularly meandering rivers (Abad et al., 2013; da Silva, 2020; Sylvester et al., 2019) and the location of their sources well within the Amazonian lowland distribution of *L. coronata* rather than in the Andes, factors that could facilitate dispersal across and around these rivers, respectively. Across several headwater regions, including those of the Caquetá, Putumayo, Napo, and Marañón rivers (i.e., localities 12–14, 24–27, and 29; see Figure 1 and Supplementary Table S1 for locality numbers), we observed more similar ancestry coefficients than those we observed across wider portions of the Amazon drainage further downriver (e.g., localities 10 vs. 21–23 vs. 44–45), consistent with the prediction that gene flow across rivers is greater toward river headwaters (Figure 1). In the Ucayali headwater region, including the Tambo and Urubamba rivers, we observed a striking exception. Here, populations showed non-overlapping ancestry coefficients despite occurring on opposite banks of the Ucayali River, which is under 1 km wide in the region (inset, Figure 1).

For the DAPC, we consistently identified K = 5 as the optimal number of populations based on the BIC (Supplementary Figures S5–S8). The DAPC, by minimizing variation within these five population clusters, highlighted the large differences between populations divided by the Amazon and Ucayali rivers, pointing to the particularly important role of these rivers as biogeographic barriers (Figure 2A; Supplementary Figures S9–S12). The DAPC also clarified the high degree of similarity between the two population clusters south of the Amazon and east of the Ucayali (localities 51–66 vs. localities 42–51 and 67–83), showing that rivers such as the Yavarí, Juruá, and Purús have a smaller role as biogeographic barriers. The PCA provided further insights into genetic structure across the landscape by permitting visualization of more within-cluster genetic variation, including the notable string-like distribution

of individuals (localities 30–41) along the PC2 axis (Figure 2B; Supplementary Figures S13–S16). These individuals are consistently oriented north to south along PC2, displaying a pattern consistent with isolation by distance (Novembre & Stephens, 2008) across the topographically complex Andean foothills west of the Ucayali River. Also apparent in the PCA was the intermediate placement of the individual sampled at locality 29 between other more distant populations (i.e., localities 24–27 and 30–36). The *K*-means clustering population assignment for locality 29 was also shared with otherwise north-of-Marañón/Amazon individuals across datasets 1–4 (Figure 2; Supplementary Tables S13–S16). These findings of intermediate placement of the individual from locality 29 in the PCA and a shared population assignment with north-of-Marañón/Amazon individuals are consistent with admixture across the Marañón River, an upper tributary of the Amazon River.

The estimated effective migration surface (EEMS) analysis showed substantial variation in effective migration, a proxy for gene flow, across the western Amazon Basin (Figure 3). Areas of reduced effective migration are evident along the Amazon and Ucayali rivers, a finding consistent with our population structure analyses using sNMF, DAPC, and PCA (Figures 1 and 2). Reduced effective migration along the Juruá, Purús, and Negro rivers is also visible, although the rate is lower. Areas of increased effective migration are apparent in interfluves such as the Purús-Madeira and Amazon-Juruá. Effective migration rates in headwater regions of the Marañón, Napo, Putumayo, and Caquetá rivers were elevated relative to those along the Ucayali and Amazon rivers (Figure 3A); however, there was low support (posterior probability < 90%) for migration rates being higher than the mean migration rate for much of the area in these headwater regions (Figure 3B). Due to the interpolation of migration rate estimates across the entire range of *L. coronata* (Figure 3A), proper interpretation of the EEMS requires attention to the density and location of sampled vertices and the probability of migration rates differing from the mean migration rate (Figure 3B).

Relationships of riverine variables to population differentiation

Spearman's correlations between population differentiation (F_{ST}) of opposite-bank populations and river width (Figure 4A) and distance from the river source (Figure 4C) were significant ($p < .05$). Population differentiation and floodplain width were not correlated (Figure 4B); however, when we removed the cross-Ucayali locality pair, we found this relationship to be significant (Supplementary Figure S18B) in addition to finding significant relationships between population differentiation (F_{ST}) and river width (Supplementary Figure S18A) and distance from river source (Supplementary Figure S18C). Although the upper Ucayali is generally < 1 km wide, has a floodplain < 10 km wide, and is in the upper reaches of the Amazon drainage, it separated the most differentiated pair of opposite-bank populations (Figure 4). We suspect that the different habitat and landscape features on either side of the Ucayali contribute to the high population differentiation between opposite-bank populations (see Discussion). Although the results of these correlations are consistent with our predictions, low sample sizes for opposite-bank comparisons along individual rivers inhibit further testing of these relationships and point to the need for more coordinated sampling of opposite-bank localities.

Demographic analyses

Comparison of demographic models for cross-river populations showed support for greater levels of migration upon moving upriver along the Amazon drainage (Table 2). For populations 21 and 44, which are on opposite banks of the Amazon River (Figure 1), the no migration model received the highest support ($w_i = 0.87$ – 1.00). In each migration model for populations 21 and 44, all three migration pulses clumped within 1 year of the population divergence 4 Ma (Supplementary Table S20), explaining the minimal effect of migration on model likelihoods. For populations 17 and 42, also along the Amazon but closer to the river source, the no migration or low migration models were alternatively the best models given the data, depending on how the Akaike weights were computed (see Methods and Table 2). For populations 15 and 28, further upriver on opposite banks of the lower Napo, the medium migration model received the highest support ($w_i = 0.82$), although the high migration model received modest support ($w_i = 0.18$).

Discussion

Our study provides unprecedented resolution of the genetic structure of the Blue-capped Manakin (*L. coronata*) around Amazonian rivers and their headwater regions. We found that a biogeographic framework based on river courses is essential for understanding genetic variation in *L. coronata*: the Amazon and Ucayali rivers formed the principal barriers to gene flow, and portions of other rivers including the lower Japurá, middle Juruá, lower Putumayo, and lower Napo were associated with smaller genetic discontinuities (Figures 1–3; Supplementary Figures S1–S4). We consider this biogeographic pattern as evidence for the ongoing role of rivers in maintaining allopatry and promoting speciation in the Amazon Basin. Inferring the historical role of river barriers, however, is complicated by the fact that rivers are not fixed features on the landscape (Musher et al., 2022; Salo et al., 1986).

Amazonian river channels have been highly dynamic due to erosion and tectonics during the Quaternary (Hayakawa et al., 2010; Pärssinen et al., 1996; Pupim et al., 2019; Ruokolainen et al., 2019), which has implications for the spatial context of gene flow and speciation (Musher et al., 2022; Salo et al., 1986). For instance, paleochannels indicate that the lower Japurá River drained into the Negro River until roughly 1 kya rather than into the Amazon, where it currently drains (Ruokolainen et al., 2019), and it is possible that landscape connectivity prior to the large avulsion could help explain overlapping ancestry coefficients among populations at localities 21–23 and those in the Japurá-Negro interfluve (localities 7–11; Figure 1). However, our ability to associate specific landscape events with patterns of genetic structure is generally limited by sampling, our knowledge of the timing for landscape events and population divergences, and the likely contributions of multiple cycles of allopatry and secondary contact among river-delimited populations. We suspect that intraspecific genetic variation has been accumulating in *L. coronata* populations across a continually shifting landscape of river barriers over the course of their evolution, with the crown age of *L. coronata* estimated at 0.9–3.5 Ma (Cheviron et al., 2005; Paulo et al., 2023; Reis et al., 2020). Despite the dynamic history of Amazonian rivers, our general finding is that the boundaries between populations of *L. coronata* are

remarkably coincident with present-day river courses, and we propose this is because opposite-bank populations that come into secondary contact due to a river rearrangement or other mechanism quickly revert to a pattern where rivers delimit range boundaries.

We obtained some preliminary evidence for this rapid return of populations in secondary contact back to river-delimited populations in our recent examination of a historically documented river avulsion on the Ucayali River (Moncrieff et al., 2020). With data from the current study, we can now confirm that a population of *L. coronata* (locality 54) on land that formed the west bank of the Ucayali until a large avulsion ~240 years ago (Pärssinen et al., 1996) showed clear affinities genetically and phenotypically with east bank populations (Figure 1). This finding suggests rapid colonization of newly accessible habitat after the avulsion by east bank populations and the disappearance of remnant populations that were on the west bank prior to the avulsion. A variety of scenarios could lead to a similar return to river-delimited populations after river rearrangements or dispersal events. For instance, if the taxa form a hybrid zone, then the zone will tend to stabilize geographically in a population density trough (Barton, 1979; Hewitt, 1988), which in Amazonia is likely to be along a river barrier. Despite the strength of many river barriers, dispersal events across rivers may happen with regularity through either active dispersal such as swimming or flight (e.g., Gonzalez-Socoloske & Snarr, 2010; Nunes, 2014; Remsen & Parker, 1983) or passive dispersal such as by a change in river course (e.g., Musher et al., 2022; Rabelo et al., 2014). An evolutionary scenario involving a recent cross-river dispersal (either active or passive) and range expansion may help explain why a large river such as the Negro, which is a known barrier for 22 avian taxon pairs above its confluence with the Branco River (Naka & Brumfield, 2018; Naka et al., 2012), could appear to have a relatively small barrier effect for populations of *L. coronata* (Figures 1–3). Interestingly, the Negro River showed a more geographically extensive, albeit weak, barrier effect than the Japurá River in our EEMS analysis (Figure 3A), which contrasts with our sNMF results in which the Japurá is a more substantial barrier (Figure 1). We attribute this discrepancy to the sensitivity of the spatially explicit EEMS method to our limited sampling along the length of the lower and middle Japurá River. However, we note that where we have collected samples along the Japurá around localities 10 and 23, the EEMS analysis does show a barrier effect with high support (Figure 3B), emphasizing the importance of migration rate probabilities for proper interpretation of the migration surface.

In addition to the effects of river rearrangements, Pleistocene climate cycles may have influenced connectivity among *L. coronata* populations by shaping the geographic distribution of *terra firme* forest (Haffer, 1969), although these habitat changes were not as extensive as originally envisioned in the Pleistocene refuge hypothesis (Baker et al., 2020). Evidence from the last 250 kyr points to a relatively stable climatic environment in western Amazonia (Cheng et al., 2013) with only small-scale contractions of rainforest habitat on the periphery of this region rather than complete isolation of forest refugia during glacial maxima (Mayle et al., 2004; Sato et al., 2021). However, even modest contractions of *terra firme* forest could pull geographic distributions away from headwater regions and increase the isolation of opposite-bank populations as suggested by the “river-refuge hypothesis” (Ayes

& Clutton-Brock, 1992; Capparella, 1991; Haffer, 1997). The presence of hybridization between divergent forms in headwater regions appears to favor a scenario of secondary contact rather than in situ divergence in parapatry (Weir et al., 2015) given that forests on either side of rivers generally have similar ecological features. However, a scenario of isolation-by-distance—with gene flow connecting populations on one side of the river mouth, around the headwaters, and back to the opposite bank along the mouth—could account for a signal of genetic connectivity through headwater regions in closely related populations.

Our data suggest a general pattern of greater genetic similarity between opposite-bank populations toward headwater regions. Our correlation analyses show that the current metrics of river width, floodplain width, and distance from river source are related variables positively associated with population differentiation (Figure 4; Supplementary Figure S18). The finding of these associations despite the dynamic nature of rivers and their floodplains over the course of their history (Passos et al., 2020; Pupim et al., 2019; Ruokolainen et al., 2019; Sawakuchi et al., 2022) again highlights that population genetic patterns appear to often readjust rapidly to current configurations of river barriers in the Amazon Basin. Although the correlation analyses show a consistent signal, they were based on seven to eight locality pairs, so further coordinated sampling on opposite banks, including along the Putumayo and Yavarí rivers which form international borders, is a high priority for future work. Demographic modeling along three sections of the Amazon drainage also supported the hypothesis of greater gene flow toward headwaters (Table 2), although further sampling is needed to extend these analyses along greater portions of the Amazon drainage.

Our sNMF analyses highlighted a few headwater regions as likely areas of genetic connectivity, particularly where the Napo, Putumayo, and Caquetá rivers approach the foothills of the Andes (Figure 1). More broadly, the swath of localities from the north bank of the Caquetá to the south bank of the Marañón (localities 12–14 and 24–29), showed more similar ancestry coefficients than populations across downstream portions of these rivers (Figure 1; localities 10 vs. 21–23 vs. 44–45). Given that the north-of-Amazon populations clustered near each other in the DAPC (Figure 2A) and PCA (Figure 2B) and thus are closely related, we suggest that future work could test the extent to which isolation by distance shaped by river barriers rather than allopatry and secondary contact in headwater regions can explain spatial patterns of genetic structure. With improved sampling along the lengths of these rivers, particularly in Colombia, it would be possible to better assess this hypothesis.

The headwater region along the Marañón River held the most divergent opposite-bank populations where we still observed evidence of gene flow. For the individual at locality 29, the intermediate ancestry coefficients (Figure 1), clustering assignment to north-bank populations (Figure 2A), and intermediate placement in the PCA (Figure 2B) highlight the Marañón as a possible region with headwater gene flow between otherwise well-differentiated populations found on either side of the Marañón/Amazon River barrier. This suggestion of connectivity is also consistent with the presence of males having dark-green plumage on the north bank of the Marañón River—the only area north of the Marañón/Amazon River barrier where greenish phenotypes occur (Figure 1; Moncrieff et al., 2022). These males with dark-green plumage

are much darker than *Lepidothrix coronata exquisita* and represent an intermediate phenotype between *L. c. exquisita* and *Lepidothrix c. coronata* (see [Supplementary Figure S14](#) in [Moncrieff et al., 2022](#)). Further genetic sampling on both sides of the Marañón will be important for gauging the presence of gene flow between *L. c. coronata* to the north and *L. c. exquisita* to the south. We have previously observed that “true” *L. c. exquisita* populations, with their characteristic bright yellow bellies and sky-blue crowns, are restricted to foothills in central Peru further south ([Moncrieff et al., 2022](#)), so we also consider the darker plumage of *L. c. exquisita* populations on the south bank of the Marañón River as evidence of gene flow from northern *L. c. coronata*. We note, however, that plumage variation in *L. coronata* is often unassociated with the major population genetic boundaries identified in our study. For instance, *L. c. coronata* and *Lepidothrix c. caelestipileata* replace each other across the middle Juruá River (localities 49 and 70, respectively) without signs of plumage intergradation ([Del-Rio et al., 2021](#)), yet the divergence between these populations is small compared to the major axes of divergence across the Amazon and Ucayali rivers ([Figures 1–4](#)). Similarly, transitions between these two taxa occur within the Juruá-Purús and Purús-Madeira interfluves with a minimal effect on ancestry coefficients ([Figure 1](#)). Populations traditionally considered *L. c. caelestipileata* vary substantially in crown color in southwest Amazonia east of the Ucayali River ([Guilherme, 2022](#)), with some populations having crown color that approaches the sky-blue of “true” *L. c. exquisita* yet showing duller yellow bellies. Despite this notable crown color variation, we did not find it to be associated with the broad patterns of genetic structure identified in this study ([Figures 1–3](#)). In summary, *L. coronata* plumage variation is complex, and further research into the spatial relationship of plumage color loci versus the rest of the genome will be important for deciphering this complexity.

Despite evidence of increased genetic connectivity across several headwater regions, we found a striking exception across the upper Ucayali River, where ancestry coefficients did not overlap ([Figure 1](#)) and where population differentiation exceeded that found across all other rivers including the Amazon ([Figure 4](#)). Prior to recent work, the upper Ucayali River appeared to be one of the most likely regions for documenting headwater gene flow due to the presence of three subspecific forms in close proximity: *L. c. exquisita* west of the Ucayali, *L. c. coronata* in the central Amazon of Peru, and the intermediate-looking *L. c. caelestipileata* in southeastern Peru. [Moncrieff et al. \(2020\)](#) collected 81 individuals along the Tambo and Urubamba rivers that showed a smooth phenotypic transition east of the Ucayali and Urubamba rivers from *L. c. coronata* towards *L. c. caelestipileata*-like populations (localities 59–65; see [Figure 1](#) inset and [Supplementary Figure S13](#) in [Moncrieff et al., 2022](#)), but a substantial plumage difference between these forms and the brighter *L. c. exquisita* west of the Ucayali and Tambo rivers ([Supplementary Figure S20](#)). This suggests the presence of gene flow among populations east of the Ucayali but not across the Ucayali, a finding further supported by the genetic structure across the Ucayali identified in this study ([Figures 1–4](#)). We suspect that several factors may be involved in this lack of genetic connectivity between populations across the Ucayali headwater region. First, [Moncrieff et al. \(2020\)](#) were unable to document any individuals in apparently suitable *terra firme* forest in the Tambo-Urubamba interfluve despite 9 field days using

extensive audio playback. Absence of a population of *L. coronata* is difficult to confirm for such a poorly known area, but it seems likely that any population of *L. coronata* within the interfluve is of low density. We also failed to detect individuals along both banks of the Huallaga River just north of locality 30 ([Figure 1](#)) despite extensive passive netting in *terra firme* forest ([Moncrieff et al., 2019](#)). These two cases of failing to detect *L. c. exquisita* in *terra firme* west of the Ucayali River may indicate this form prefers foothill forest rather than lowland *terra firme* forest such as occupied by *L. c. coronata* and *L. c. caelestipileata* east of the Ucayali. If contact does occur between forms in the Ucayali headwater region, then we suspect it would involve very limited, if any, gene flow given that we did not detect admixture. Although vocalizations are very similar among these subspecies, it seems possible that plumage differences between *L. c. exquisita* and other forms could promote assortative mating in the Ucayali headwater region. Alternatively, possible habitat preferences—foothill forest for *L. c. exquisita* and *terra firme* forest for *L. c. coronata* and *L. c. caelestipileata*—could limit contact between subspecific forms if the transition between the two habitats is not suitable for any subspecies. Elevating *L. c. exquisita* to a species-level taxon, however, seems unwarranted at present given the need for further sampling for possible contact with other forms in the Ucayali headwater region. In addition, *L. c. exquisita* intergrades in plumage with *L. c. coronata* along the Marañón River ([Moncrieff et al., 2022](#)), and our genetic analyses suggest admixture across this barrier ([Figures 1 and 2](#)). Further sampling of the contact zone along the Marañón River is a high priority for future work.

In conclusion, our data suggest that genetic connectivity is elevated across several headwater regions, which provides some support for a traditional critique of the riverine barrier hypothesis that headwater gene flow can limit the role of rivers as barriers and drivers of diversification in the Amazon Basin ([Haffer, 1997](#); [Moritz et al., 2000](#)). However, we do not consider gene flow across narrow rivers in headwater regions as a fundamental weakness of the riverine barrier hypothesis, which maintains its broad explanatory power, but rather a finding that helps to refine the hypothesis. Even in the case of continuous headwater gene flow, we suspect that isolation by distance could lead to the accumulation of distinct genotypes on opposite banks of lower portions of rivers. A rearrangement along the lower portion of a river could then easily place distinct genotypes into contact and simultaneously isolate the passively transferred population from closely related populations. This type of scenario, without invoking any climate-related factors, could promote speciation ([Musher et al., 2022](#)). The river-refuge hypothesis has the advantage of invoking climatic habitat shifts ([Ayles & Clutton-Brock, 1992](#); [Capparella, 1991](#); [Haffer, 1997](#)), which may have influenced species- and subspecies-level diversification during the Pleistocene, but historically this hypothesis has not recognized the importance of cross-river dispersal and river rearrangements in accounting for observed patterns in Amazonian biogeography. We suggest expanding the flexibility of the riverine barrier hypothesis to acknowledge the contributions of cross-river dispersal, river rearrangements, and modest habitat shifts during the Pleistocene. In this broader framework, the riverine barrier hypothesis would highlight the important role of rivers in driving speciation and maintaining biodiversity in the Amazon Basin while also acknowledging the complex array of behavioral, landscape, and climatic forces

working on and around these barriers. The spatial patterns of genetic variation that we identified across Amazonian rivers and their headwater regions have particular relevance to the Amazonian taxa of *terra firme* forests, including over 1,000 species of birds (Parker, 1996). Variability in life history traits such as dispersal ability, ancestral range, affinity for *terra firme* forest, and tolerance of light gaps all likely contribute to incongruent divergence times for populations found across river barriers (Smith et al., 2014), yet genetic structure across many of the largest Amazonian rivers remains an important theme in Amazonian biogeography. We suspect that the evidence in *L. coronata* for greater genetic connectivity across multiple headwater regions may find broad replicability in other *terra firme* taxa, although more studies with extensive sampling in headwater regions will be necessary to adequately test this idea.

Supplementary material

Supplementary material is available online at *Evolution*.

Data availability

Raw reads are stored in the NCBI Sequence Read Archive under BioProjects PRJNA782327 and PRJNA787238. VCF datasets, custom scripts, and input/output for EEMS, sNMF, F_{ST} , and momi analyses are archived in the Dryad Digital Repository (<https://doi.org/10.5061/dryad.5tb2rbp9s>).

Author contributions

A.E.M., R.T.B., and B.C.F. conceived the study. A.E.M., A.E.H., C.F., A.P.C., A.A., and T.V. collected samples. A.E.M. and R.C.R. conducted lab work. A.E.M. conducted analyses and wrote the manuscript with contributions from all co-authors.

Funding

For fieldwork, we received funding from the Coypu Foundation and LSUMNS Tropical Bird Research Fund. Laboratory supplies and sequencing were funded by an American Ornithological Society Alexander Wetmore Memorial Research Award and an American Society of Naturalists Student Research Award to A.E.M., National Science Foundation (NSF) grant DEB-1146265 to R.T.B., and DEB-1655624 to R.T.B. and B.C.F. A.E.M. and A.E.H. also received support from NSF Graduate Research Fellowships during this project.

Conflict of interest: The authors declare no conflict of interest.

Acknowledgments

We thank Michael Whitlock, Van Remsen, Gregory Thom, Jessica Eberhard, Michael Hellberg, and three anonymous reviewers for their constructive comments that improved the manuscript. Joel Peña and Jessie Salter assisted with laboratory work, and Scott Herke at the LSU Genomics Facility helped with genomic sample quality control. Subir Shakya provided *Lepidothrix coronata* artwork, and Victor Gamarra provided photographs of *L. coronata* that guided

our selection of field sites in Peru. We thank the following institutions for providing the tissue and/or toepad samples for this project: American Museum of Natural History (Joel Cracraft, Paul Sweet, Tom Trombone, and Peter Capainolo), Academy of Natural Sciences of Drexel University (Jason Weckstein, Nate Rice), Field Museum of Natural History (Shannon Hackett, John Bates, and Ben Marks), Louisiana State University Museum of Natural Science (Fred Sheldon, Donna Dittmann), Museu Paraense Emílio Goeldi (Fátima Lima), and Museum of Southwestern Biology (Chris Witt, Mariel Campbell). Portions of this research were conducted with high-performance computational resources provided by Louisiana State University (<http://www.hpc.lsu.edu>). Field assistants Edgar Monsín, Elizabeth Andrade, and Juan Hueroné helped us complete fieldwork in Peru. We are also grateful for the support of the Central Asháninka de Río Tambo (CART) and Organización Distrital Indígena de Masisa (ORDIM) and the Peruvian indigenous communities of Camisea, Cushireni, Mayapo, Nuevo San Martín, Preferida de Charasmaná, Sepahua, and Serjali. All specimen collection in Peru was authorized by the Servicio Nacional Forestal y de Fauna Silvestre (SERFOR) under permits 203-2015-SERFOR-DGGSPFFS and 222-2015-SERFOR-DGGSPFFS. Specimen collection was carried out under LSU's Institutional Animal Care and Use Committee (IACUC) protocol numbers 15-036 and 18-054.

References

- Abad, J. D., Vizcarra, J., Paredes, J., Montoro, H., & Frias, C. (2013, July 17–19). *Morphodynamics of the upper Peruvian Amazonian rivers, implications into fluvial transportation*. Paper presented at International Conference IDS2013—Amazonia, Iquitos, Peru. <https://www.openstarts.units.it/handle/10077/8822>
- Akaike, H. (1974). A new look at the statistical model identification. *IEEE Transactions on Automatic Control*, 19(6), 716–723. <https://doi.org/10.1109/tac.1974.1100705>
- Aleixo, A. (2004). Historical diversification of a *terra-firme* forest bird superspecies: A phylogeographic perspective on the role of different hypotheses of Amazonian diversification. *Evolution*, 58(6), 1303–1317. <https://doi.org/10.1111/j.0014-3820.2004.tb01709.x>
- Anthony, N. M., Johnson-Bawe, M., Jeffery, K., Clifford, S. L., Abernethy, K. A., Tutin, C. E., Lahm, S. A., White, L. J. T., Utley, J. F., Wickings, E. J., & Bruford, M. W. (2007). The role of Pleistocene refugia and rivers in shaping gorilla genetic diversity in central Africa. *Proceedings of the National Academy of Sciences*, 104(51), 20432–20436. <https://doi.org/10.1073/pnas.0704816105>
- Armenta, J. K., Weckstein, J. D., & Lane, D. F. (2005). Geographic variation in mitochondrial DNA sequences of an Amazonian nonpasserine: The Black-Spotted Barbet complex. *The Condor*, 107(3), 527–536. <https://doi.org/10.1093/condor/107.3.527>
- Ayres, J. M., & Clutton-Brock, T. H. (1992). River boundaries and species range size in Amazonian primates. *The American Naturalist*, 140(3), 531–537. <https://doi.org/10.1086/285427>
- Baker, P. A., Fritz, S. C., Battisti, D. S., Dick, C. W., Vargas, O. M., Asner, G. P., Martin, R. E., Wheatley, A., & Prates, I. (2020). Beyond refugia: New insights on Quaternary climate variation and the evolution of biotic diversity in tropical South America. In V. Rull, & A. C. Carnaval (Eds.), *Neotropical diversification: patterns and processes* (pp. 51–70). Springer International Publishing.
- Barton, N. H. (1979). The dynamics of hybrid zones. *Heredity*, 43(3), 341–359. <https://doi.org/10.1038/hdy.1979.87>
- Bayona-Vásquez, N. J., Glenn, T. C., Kieran, T. J., Pierson, T. W., Hoffberg, S. L., Scott, P. A., Bentley, K. E., Finger, J. W., Louha, S., Troendle, N., Diaz-Jaimes, P., Mauricio, R., & Faircloth, B. C. (2019). Adapterama III: Quadruple-indexed, double/triple-enzyme

- RADseq libraries (2RAD/3RAD). *PeerJ*, 7, e7724. <https://doi.org/10.7717/peerj.7724>
- Berv, J. S., Campagna, L., Feo, T. J., Castro-Astor, I., Ribas, C. C., Prum, R. O., & Lovette, I. J. (2021). Genomic phylogeography of the White-crowned Manakin *Pseudopipra pipra* (Aves: Pipridae) illuminates a continental-scale radiation out of the Andes. *Molecular Phylogenetics and Evolution*, 164, 107205. <https://doi.org/10.1016/j.ympev.2021.107205>
- Brant, S. V., & Ortí, G. (2003). Phylogeography of the northern short-tailed shrew, *Blarina brevicauda* (Insectivora: Soricidae): Past fragmentation and postglacial recolonization. *Molecular Ecology*, 12(6), 1435–1449. <https://doi.org/10.1046/j.1365-294x.2003.01789.x>
- Brumfield, R. T. (2012). Inferring the origins of lowland Neotropical birds. *The Auk*, 129(3), 367–376. <https://doi.org/10.1525/auk.2012.129.3.367>
- Burney, C. W., & Brumfield, R. T. (2009). Ecology predicts levels of genetic differentiation in Neotropical birds. *The American Naturalist*, 174(3), 358–368. <https://doi.org/10.1086/603613>
- Burnham, K., & Anderson, D. (2002). *Model selection and multi-model inference. A practical information-theoretic approach* (2nd ed.). Springer-Verlag.
- Bushnell, B. (2014). *BBMap: A fast, accurate, splice-aware aligner*. Lawrence Berkeley National Lab (LBNL).
- Capparella, A. P. (1987). *Effects of riverine barriers on genetic differentiation of Amazonian forest undergrowth birds [Doctoral dissertation]*. LSU Scholarly Repository. https://repository.lsu.edu/gradschool_disstheses/4346
- Capparella, A. P. (1988). Genetic variation in Neotropical birds: Implications for the speciation process. In H. Ouellet (Ed.), *Acta XIX Congressus Internationalis Ornithologici* (pp. 1658–1664). University of Ottawa Press.
- Capparella, A. P. (1991). Neotropical avian diversity and riverine barriers. In B. D. Bell, R. O. Cossee, J. E. C. Flux, B. D. Heather, R. A. Hitchmough, C. J. R. Robertson, & M. J. Williams (Eds.), *Acta XX Congressus Internationalis Ornithologici* (pp. 307–316). Huthcheson, Bowman, & Stewart Ltd.
- Catchen, J., Hohenlohe, P. A., Bassham, S., Amores, A., & Cresko, W. A. (2013). Stacks: An analysis tool set for population genomics. *Molecular Ecology*, 22(11), 3124–3140. <https://doi.org/10.1111/mec.12354>
- Cheng, H., Sinha, A., Cruz, F. W., Wang, X., Edwards, R. L., d'Horta, F. M., Ribas, C. C., Vuille, M., Stott, L. D., & Auler, A. S. (2013). Climate change patterns in Amazonia and biodiversity. *Nature Communications*, 4, 1411. <https://doi.org/10.1038/ncomms2415>
- Chevron, Z. A., Hackett, S. J., & Capparella, A. P. (2005). Complex evolutionary history of a Neotropical lowland forest bird (*Lepidothrix coronata*) and its implications for historical hypotheses of the origin of Neotropical avian diversity. *Molecular Phylogenetics and Evolution*, 36(2), 338–357. <https://doi.org/10.1016/j.ympev.2005.01.015>
- Collen, B., Whitton, F., Dyer, E. E., Baillie, J. E. M., Cumberlidge, N., Darwall, W. R. T., Pollock, C., Richman, N. I., Soulsby, A. -M., & Böhm, M. (2014). Global patterns of freshwater species diversity, threat and endemism. *Global Ecology and Biogeography*, 23(1), 40–51. <https://doi.org/10.1111/geb.12096>
- Cortés-Ortiz, L., Bermingham, E., Rico, C., Rodríguez-Luna, E., Sampaio, I., & Ruiz-García, M. (2003). Molecular systematics and biogeography of the Neotropical monkey genus, *Alouatta*. *Molecular Phylogenetics and Evolution*, 26(1), 64–81. [https://doi.org/10.1016/s1055-7903\(02\)00308-1](https://doi.org/10.1016/s1055-7903(02)00308-1)
- Cracraft, J. (1985). Historical biogeography and patterns of differentiation within the South American avifauna: areas of endemism. *Ornithological Monographs*, 36, 49–84. <https://doi.org/10.2307/40168278>
- d'Horta, F. M., Cuervo, A. M., Ribas, C. C., Brumfield, R. T., & Miyaki, C. Y. (2013). Phylogeny and comparative phylogeography of *Sclerurus* (Aves: Furnariidae) reveal constant and cryptic diversification in an old radiation of rain forest understorey specialists. *Journal of Biogeography*, 40(1), 37–49. <https://doi.org/10.1111/j.1365-2699.2012.02760.x>
- da Silva, P. J. M. (2020). Channel pattern and flow rate analyses of the Juruá River, northwest of Brasil. *Revista de Geologia*, 33(1), 103–110.
- Danecek, P., Auton, A., Abecasis, G., Albers, C. A., Banks, E., DePristo, M. A., Handsaker, R. E., Lunter, G., Marth, G. T., Sherry, S. T., McVean, G., & Durbin, R.; 1000 Genomes Project Analysis Group. (2011). The variant call format and VCFtools. *Bioinformatics*, 27(15), 2156–2158. <https://doi.org/10.1093/bioinformatics/btr330>
- Del-Rio, G., Mutchler, M. J., Costa, B., Hiller, A. E., Lima, G., Matinata, B., Salter, J. F., Silveira, L. F., Rego, M. A., & Schmitt, D. C. (2021). Birds of the Juruá River: Extensive várzea forest as a barrier to terra firme birds. *Journal of Ornithology*, 162(2), 565–577. <https://doi.org/10.1007/s10336-020-01850-0>
- Dias-Terceiro, R. G., Kaefer, I. L., de Fraga, R., de Araújo, M. C., Simões, P. I., & Lima, A. P. (2015). A matter of scale: Historical and environmental factors structure anuran assemblages from the upper Madeira River, Amazonia. *Biotropica*, 47(2), 259–266. <https://doi.org/10.1111/btp.12197>
- Eriksson, J., Hohmann, G., Boesch, C., & Vigilant, L. (2004). Rivers influence the population genetic structure of bonobos (*Pan paniscus*). *Molecular Ecology*, 13(11), 3425–3435. <https://doi.org/10.1111/j.1365-294X.2004.02332.x>
- Fernandes, A. M., Wink, M., Sardelli, C. H., & Aleixo, A. (2014). Multiple speciation across the Andes and throughout Amazonia: The case of the spot-backed antbird species complex (*Hylophylax naevius/Hylophylax naevioides*). *Journal of Biogeography*, 41(6), 1094–1104. <https://doi.org/10.1111/jbi.12277>
- Fouquet, A., Courtois, E. A., Baudain, D., Lima, J. D., Souza, S. M., Noonan, B. P., & Rodrigues, M. T. (2015). The trans-riverine genetic structure of 28 Amazonian frog species is dependent on life history. *Journal of Tropical Ecology*, 31(4), 361–373. <https://doi.org/10.1017/s0266467415000206>
- Frichot, E., & François, O. (2015). LEA: An R package for landscape and ecological association studies. *Methods in Ecology and Evolution*, 6(8), 925–929. <https://doi.org/10.1111/2041-210x.12382>
- Frichot, E., Mathieu, F., Trouillon, T., Bouchard, G., & François, O. (2014). Fast and efficient estimation of individual ancestry coefficients. *Genetics*, 196(4), 973–983. <https://doi.org/10.1534/genetics.113.160572>
- Gascon, C., Malcolm, J. R., Patton, J. L., da Silva, M. N., Bogart, J. P., Loughheed, S. C., Peres, C. A., Neckel, S., & Boag, P. T. (2000). Riverine barriers and the geographic distribution of Amazonian species. *Proceedings of the National Academy of Sciences of the United States of America*, 97(25), 13672–13677. <https://doi.org/10.1073/pnas.230136397>
- Gentry, A. H. (1988). Tree species richness of upper Amazonian forests. *Proceedings of the National Academy of Sciences of the United States of America*, 85(1), 156–159. <https://doi.org/10.1073/pnas.85.1.156>
- Gibbs, R. J. (1967). The geochemistry of the Amazon River system: Part I. The factors that control the salinity and the composition and concentration of the suspended solids. *Geological Society of America Bulletin*, 78(10), 1203–1232. [https://doi.org/10.1130/0016-7606\(1967\)78\[1203:tgotar\]2.0.co;2](https://doi.org/10.1130/0016-7606(1967)78[1203:tgotar]2.0.co;2)
- Glenn, T. C., Nilsen, R. A., Kieran, T. J., Sanders, J. G., Bayona-Vásquez, N. J., Finger, J. W., Pierson, T. W., Bentley, K. E., Hoffberg, S. L., Louha, S., Garcia-De Leon, F. J., Del Rio Portilla, M. A., Reed, K. D., Anderson, J. L., Meece, J. K., Aggrey, S. E., Rekaya, R., Alabady, M., Belanger, M., ... Faircloth, B. C. (2019). Adapterama I: Universal stubs and primers for 384 unique dual-indexed or 147,456 combinatorially-indexed Illumina libraries (iTru & iNext). *PeerJ*, 7, e7755. <https://doi.org/10.7717/peerj.7755>
- Godinho, M. B. de C., & da Silva, F. R. (2018). The influence of riverine barriers, climate, and topography on the biogeographic regionalization of Amazonian anurans. *Scientific Reports*, 8(1), 3427. <https://doi.org/10.1038/s41598-018-21879-9>

- Gonzalez-Socoloske, D., & Snarr, K. A. (2010). An incident of swimming in a large river by a mantled howling monkey (*Alouatta palliata*) on the north coast of Honduras. *Neotropical Primates*, 17(1), 28–31. <https://doi.org/10.1896/044.017.0102>
- Guilherme, E. (2016). *Aves do Acre*. Edufac (Editora da Universidade Federal do Acre).
- Guilherme, E. (2022). On the sympatric occurrence of two subspecies of Blue-crowned Manakin, *Lepidothrix coronata exquisita* and *L. c. caelestipileata*, in south-west Amazonia. *Bulletin of the British Ornithologists' Club*, 142(3), 323–328. <https://doi.org/10.25226/bboc.v142i3.2022.a5>
- Haffer, J. (1969). Speciation in Amazonian forest birds. *Science*, 165(3889), 131–137. <https://doi.org/10.1126/science.165.3889.131>
- Haffer, J. (1970). Art-Entstehung bei einigen Waldvögeln Amazoniens. *Journal Für Ornithologie*, 111, 285–331. <https://doi.org/10.1007/bf01653396>
- Haffer, J. (1992). On the “river effect” in some forest birds of southern Amazonia. *Boletim Do Museu Paraense Emílio Goeldi Serie Zoologia*, 8, 217–245.
- Haffer, J. (1997). Alternative models of vertebrate speciation in Amazonia: An overview. *Biodiversity and Conservation*, 6(3), 451–476. <https://doi.org/10.1023/A:1018320925954>
- Hall, J. P. W., & Harvey, D. J. (2002). The phylogeography of Amazonia revisited: New evidence from riordinid butterflies. *Evolution*, 56(7), 1489–1497. [https://doi.org/10.1554/0014-3820\(2002\)056\[1489:tpoarn\]2.0.co;2](https://doi.org/10.1554/0014-3820(2002)056[1489:tpoarn]2.0.co;2)
- Hayakawa, E. H., Rossetti, D. F., & Valeriano, M. M. (2010). Applying DEM-SRTM for reconstructing a late Quaternary paleodrainage in Amazonia. *Earth and Planetary Science Letters*, 297(1–2), 262–270. <https://doi.org/10.1016/j.epsl.2010.06.028>
- Hayes, F. E., & Sewlal, J. N. (2004). The Amazon River as a dispersal barrier to passerine birds: Effects of river width, habitat and taxonomy. *Journal of Biogeography*, 31(11), 1809–1818. <https://doi.org/10.1111/j.1365-2699.2004.01139.x>
- Hess, L. L., Melack, J. M., Affonso, A. G., Barbosa, C. C. F., Gastil-Buhl, M., & Novo, E. M. L. M. (2015). *LBA-ECO LC-07 Wetland extent, vegetation, and inundation: Lowland Amazon Basin*. ORNL DAAC. <https://doi.org/10.3334/ORNLDAAC/1284>
- Hewitt, G. M. (1988). Hybrid zones—natural laboratories for evolutionary studies. *Trends in Ecology & Evolution*, 3(7), 158–167. [https://doi.org/10.1016/0169-5347\(88\)90033-X](https://doi.org/10.1016/0169-5347(88)90033-X)
- Hoffberg, S. L., Kieran, T. J., Catchen, J. M., Devault, A., Faircloth, B. C., Mauricio, R., & Glenn, T. C. (2016). RADcap: Sequence capture of dual-digest RADseq libraries with identifiable duplicates and reduced missing data. *Molecular Ecology Resources*, 16(5), 1264–1278. <https://doi.org/10.1111/1755-0998.12566>
- Hortal, J., de Bello, F., Diniz-Filho, J. A. F., Lewinsohn, T. M., Lobo, J. M., & Ladle, R. J. (2015). Seven shortfalls that beset large-scale knowledge of biodiversity. *Annual Review of Ecology, Evolution, and Systematics*, 46(1), 523–549. <https://doi.org/10.1146/annurev-ecolsys-112414-054400>
- Hurvich, C. M., & Tsai, C.-L. (1989). Regression and time series model selection in small samples. *Biometrika*, 76(2), 297–307. <https://doi.org/10.1093/biomet/76.2.297>
- Jackson, N. D., & Austin, C. C. (2010). The combined effects of rivers and refugia generate extreme cryptic fragmentation within the common ground skink (*Scincella lateralis*). *Evolution*, 64(2), 409–428. <https://doi.org/10.1111/j.1558-5646.2009.00840.x>
- Jalil, M. F., Cable, J., Sinyor, J., Lackman-Ancrenaz, I., Ancrenaz, M., Bruford, M. W., & Goossens, B. (2008). Riverine effects on mitochondrial structure of Bornean orangutans (*Pongo pygmaeus*) at two spatial scales. *Molecular Ecology*, 17(12), 2898–2909. <https://doi.org/10.1111/j.1365-294X.2008.03793.x>
- Jenkins, C. N., Pimm, S. L., & Joppa, L. N. (2013). Global patterns of terrestrial vertebrate diversity and conservation. *Proceedings of the National Academy of Sciences of the United States of America*, 110(28), E2602–E2610. <https://doi.org/10.1073/pnas.1302251110>
- Johnson, O., Howard, J. T., & Brumfield, R. T. (2021). Systematics of a Neotropical clade of dead-leaf-foraging antwrens (Aves: Thamnophilidae; *Epinecrophylla*). *Molecular Phylogenetics and Evolution*, 154, 106962. <https://doi.org/10.1016/j.ympev.2020.106962>
- Jombart, T., & Ahmed, I. (2011). ADEGENET 1.3-1: New tools for the analysis of genome-wide SNP data. *Bioinformatics*, 27(21), 3070–3071. <https://doi.org/10.1093/bioinformatics/btr521>
- Jombart, T., Devillard, S., & Balloux, F. (2010). Discriminant analysis of principal components: A new method for the analysis of genetically structured populations. *BMC Genetics*, 11, 94. <https://doi.org/10.1186/1471-2156-11-94>
- Kamm, J., Terhorst, J., Durbin, R., & Song, Y. S. (2020). Efficiently inferring the demographic history of many populations with allele count data. *Journal of the American Statistical Association*, 115(531), 1472–1487. <https://doi.org/10.1080/01621459.2019.1635482>
- Kopelman, N. M., Mayzel, J., Jakobsson, M., Rosenberg, N. A., & Mayrose, I. (2015). CLUMPAK: A program for identifying clustering modes and packaging population structure inferences across K. *Molecular Ecology Resources*, 15(5), 1179–1191. <https://doi.org/10.1111/1755-0998.12387>
- Lane, D. F., Pequeño, T., & Flores Villar, J. (2003). Birds. In N. Pitman, C. Vriesendorp, & D. Moskovits (Eds.), *Perú: Yavari. Rapid Biological Inventories Report 11* (pp. 150–156). Field Museum of Natural History.
- Leaché, A. D., & Reeder, T. W. (2002). Molecular systematics of the eastern fence lizard (*Sceloporus undulatus*): A comparison of parsimony, likelihood, and Bayesian approaches. *Systematic Biology*, 51(1), 44–68. <https://doi.org/10.1080/106351502753475871>
- Leite, R. N., & Rogers, D. S. (2013). Revisiting Amazonian phylogeography: Insights into diversification hypotheses and novel perspectives. *Organisms Diversity & Evolution*, 13(4), 639–664. <https://doi.org/10.1007/s13127-013-0140-8>
- Li, H., & Durbin, R. (2009). Fast and accurate short read alignment with Burrows-Wheeler transform. *Bioinformatics*, 25(14), 1754–1760. <https://doi.org/10.1093/bioinformatics/btp324>
- Li, H., Handsaker, B., Wysoker, A., Fennell, T., Ruan, J., Homer, N., Marth, G., Abecasis, G., & Durbin, R.; 1000 Genome Project Data Processing Subgroup. (2009). The sequence Alignment/Map format and SAMtools. *Bioinformatics*, 25(16), 2078–2079. <https://doi.org/10.1093/bioinformatics/btp352>
- Lomolino, M. V. (2004). Conservation biogeography. In M. V. Lomolino & L. R. Heaney (Eds.), *Frontiers of biogeography: New directions in the geography of nature* (pp. 293–296). Sinauer Associates.
- Luna, L. W., Ribas, C. C., & Aleixo, A. (2022). Genomic differentiation with gene flow in a widespread Amazonian floodplain-specialist bird species. *Journal of Biogeography*, 49(9), 1670–1682. <https://doi.org/10.1111/jbi.14257>
- Mayle, F. E., Beerling, D. J., Gosling, W. D., & Bush, M. B. (2004). Responses of Amazonian ecosystems to climatic and atmospheric carbon dioxide changes since the last glacial maximum. *Philosophical Transactions of the Royal Society of London, Series B: Biological Sciences*, 359(1443), 499–514. <https://doi.org/10.1098/rstb.2003.1434>
- Moncrieff, A. E., Faircloth, B. C., & Brumfield, R. T. (2022). Systematics of *Lepidothrix* manakins (Aves: Passeriformes: Pipridae) using RADcap markers. *Molecular Phylogenetics and Evolution*, 173, 107525. <https://doi.org/10.1016/j.ympev.2022.107525>
- Moncrieff, A. E., Johnson, O., Felix, C., Hiller, A. E., Corbett, E. C., Brady, M. L., Seeholzer, G. F., Bautista, E., Lane, D. F., & Harvey, M. G. (2020). Avifaunal surveys in the central Peruvian Amazon clarify range limits and highlight links between avian and habitat diversity. *The Wilson Journal of Ornithology*, 132(4), 934–951. <https://doi.org/10.1676/20-00082>
- Moncrieff, A. E., Johnson, O., Lane, D. F., Álvarez A, J., Balta, K., Eckhardt, K., Armenta, J., Valqui, T., Hernández, F., Soto Huaira, M., Mur, C., Harvey, M. G., Verde-Guerra, K., & Figueroa Ramírez, S. (2019). Avifaunal surveys along the lower Huallaga River, Region of Loreto, Peru: New distributional records, collection of

- topotypes, and taxonomic implications. *The Wilson Journal of Ornithology*, 131, 486–501. <https://doi.org/10.1676/18-108>
- Moraes, L. J. C. L., Pavan, D., Barros, M. C., & Ribas, C. C. (2016). The combined influence of riverine barriers and flooding gradients on biogeographical patterns for amphibians and squamates in south-eastern Amazonia. *Journal of Biogeography*, 43(11), 2113–2124. <https://doi.org/10.1111/jbi.12756>
- Moritz, C., Patton, J. L., Schneider, C. J., & Smith, T. B. (2000). Diversification of rainforest faunas: an integrated molecular approach. *Annual Review of Ecology and Systematics*, 31(1), 533–563. <https://doi.org/10.1146/annurev.ecolsys.31.1.533>
- Musher, L. J., Giakoumis, M., Albert, J., Del-Rio, G., Rego, M., Thom, G., Aleixo, A., Ribas, C. C., Brumfield, R. T., Smith, B. T., & Cracraft, J. (2022). River network rearrangements promote speciation in lowland Amazonian birds. *Science Advances*, 8(14), eabn1099. <https://doi.org/10.1126/sciadv.abn1099>
- Nadachowska-Brzyska, K., Li, C., Smeds, L., Zhang, G., & Ellegren, H. (2015). Temporal dynamics of avian populations during Pleistocene revealed by whole-genome sequences. *Current Biology*, 25(10), 1375–1380. <https://doi.org/10.1016/j.cub.2015.03.047>
- Naka, L. N., Bechtoldt, C. L., Henriques, L., & Brumfield, R. T. (2012). The role of physical barriers in the location of avian suture zones in the Guiana Shield, northern Amazonia. *The American Naturalist*, 179(4), E115–E132. <https://doi.org/10.1086/664627>
- Naka, L. N., & Brumfield, R. T. (2018). The dual role of Amazonian rivers in the generation and maintenance of avian diversity. *Science Advances*, 4(8), eaar8575. <https://doi.org/10.1126/sciadv.aar8575>
- Naka, L. N., Costa, B. M., Lima, G. R., & Claramunt, S. (2022). Riverine barriers as obstacles to dispersal in Amazonian birds. *Frontiers in Ecology and Evolution*, 10, 846975. <https://doi.org/10.3389/fevo.2022.846975>
- Nazareno, A. G., Dick, C. W., & Lohmann, L. G. (2017). Wide but not impermeable: Testing the riverine barrier hypothesis for an Amazonian plant species. *Molecular Ecology*, 26(14), 3636–3648. <https://doi.org/10.1111/mec.14142>
- Nazareno, A. G., Dick, C. W., & Lohmann, L. G. (2019). A biogeographic barrier test reveals a strong genetic structure for a canopy-emergent Amazon tree species. *Scientific Reports*, 9(1), 18602. <https://doi.org/10.1038/s41598-019-55147-1>
- Norris, K. S. (1958). The evolution and systematics of the iguanid genus *Uma* and its relation to the evolution of other North American desert reptiles. *Bulletin of the American Museum of Natural History*, 114, 247–326.
- Novembre, J., & Stephens, M. (2008). Interpreting principal component analyses of spatial population genetic variation. *Nature Genetics*, 40(5), 646–649. <https://doi.org/10.1038/ng.139>
- Nunes, A. V. (2014). Report of a black spider monkey (*Ateles chamek*) swimming in a large river in central-western Brazil. *Neotropical Primates*, 21(2), 204–206. <https://doi.org/10.1896/044.021.0210>
- O'Meara, B. C., Ané, C., Sanderson, M. J., & Wainwright, P. C. (2006). Testing for different rates of continuous trait evolution using likelihood. *Evolution*, 60(5), 922–933. <https://doi.org/10.1111/j.0014-3820.2006.tb01171.x>
- Oliveira, U., Paglia, A. P., Brescovit, A. D., Carvalho, C. J. B., Silva, D. P., Rezende, D. T., Leite, F. S. F., Batista, J. A. N., Barbosa, J. P. P. P., Stehmann, J. R., Ascher, J. S., Vasconcelos, M. F., De Marco, P., Jr., Löwenberg-Neto, P., Dias, P. G., Ferro, V. G., & Santos, A. J. (2016). The strong influence of collection bias on biodiversity knowledge shortfalls of Brazilian terrestrial biodiversity. *Diversity & Distributions*, 22(12), 1232–1244. <https://doi.org/10.1111/ddi.12489>
- Oren, D. C., & Albuquerque, H. G. de (1991). Priority areas for new avian collections in Brazilian Amazonia. *Goeldiana Zoologia*, 6, 1–11.
- Parker, T. A., III. (1996). Ecological and distributional databases for Neotropical birds. In D. F. Stotz, J. W. Fitzpatrick, T. A. Parker III, & D. Moskovits (Eds.), *Neotropical birds: Ecology and conservation* (pp. 113–436). University of Chicago Press.
- Pärssinen, M. H., Salo, J. S., & Räsänen, M. E. (1996). River floodplain relocations and the abandonment of Aborigine settlements in the upper Amazon Basin: A historical case study of San Miguel de Cunibos at the middle Ucayali River. *Geoarchaeology*, 11(4), 345–359. [https://doi.org/10.1002/\(sici\)1520-6548\(199607\)11:4<345::aid-gea3>3.0.co;2-1](https://doi.org/10.1002/(sici)1520-6548(199607)11:4<345::aid-gea3>3.0.co;2-1)
- Paulo, P., Teófilo, F. H., Bertuol, C., Polo, E., Moncrieff, A. E., Bandeira, L. N., Nuñez-Penichet, C., Fernandes, I. Y., Bosholn, M., Machado, A. F., Luna, L. W., Peçanha, W. T., Rampini, A. P., Hashimoto, S., Dias, C., Araripe, J., Aleixo, A., do Rêgo, P. S., Hrbek, T., ... Anciães, M. (2023). Geographic drivers of genetic and plumage color diversity in the blue-crowned manakin. *Evolutionary Biology*, 50, 413–431. <https://doi.org/10.1007/s11692-023-09613-4>
- Peres, C. A., Patton, J. L., & da Silva, M. N. (1996). Riverine barriers and gene flow in Amazonian saddle-back tamarins. *Folia Primatologica*, 67(3), 113–124. <https://doi.org/10.1159/000157213>
- Petkova, D. (2016). *Str2diffs: Read genetic data in structure format, compute diffs matrix*. <https://github.com/dipetkov/eems/tree/master/str2diffs>
- Petkova, D. (2017). *Instruction Manual. EMS: A method to visualize patterns of non-stationary isolation by distance. Version 0.0.0.9000*. <https://github.com/dipetkov/eems/blob/master/Documentation/EEMS-doc.pdf>
- Petkova, D., Novembre, J., & Stephens, M. (2016). Visualizing spatial population structure with estimated effective migration surfaces. *Nature Genetics*, 48(1), 94–100. <https://doi.org/10.1038/ng.3464>
- Passos, M. S., Soares, E. A. A., Tatum, S. H., Yee, M., Mittani, J. C. R., Hayakawa, E. H., & Salazar, C. A. (2020). Pleistocene-Holocene sedimentary deposits of the Solimões-Amazonas fluvial system, Western Amazonia. *Journal of South American Earth Sciences*, 98, 102455. <https://doi.org/10.1016/j.jsames.2019.102455>
- Posada, D., & Crandall, K. A. (2001). Selecting the best-fit model of nucleotide substitution. *Systematic Biology*, 50(4), 580–601. <https://doi.org/10.1080/10635150118469>
- Pupim, F. N., Sawakuchi, A. O., Almeida, R. P., Ribas, C. C., Kern, A. K., Hartmann, G. A., Chiessi, C. M., Tamura, L. N., Mineli, T. D., Savian, J. F., Grohmann, C. H., Bertassoli, D. J., Stern, A. G., Cruz, F. W., & Cracraft, J. (2019). Chronology of terra firme formation in Amazonian lowlands reveals a dynamic Quaternary landscape. *Quaternary Science Reviews*, 210, 154–163. <https://doi.org/10.1016/j.quascirev.2019.03.008>
- QGIS.org. (2021). *QGIS Geographic Information System*. QGIS Association. <https://www.qgis.org/>
- R Core Team. (2021). *R: A language and environment for statistical computing*. R Foundation for Statistical Computing. <https://www.R-project.org/>
- Rabelo, R. M., Silva, F. E., Vieira, T., Ferreira-Ferreira, J., Paim, F. P., Dutra, W., de Souza e Silva Júnior, J., & Valsecchi, J. (2014). Extension of the geographic range of *Ateles chamek* (Primates, Atelidae): Evidence of river-barrier crossing by an Amazonian primate. *Primates*, 55(2), 167–171. <https://doi.org/10.1007/s10329-014-0409-3>
- Rego, M. A., Del-Rio, G., & Brumfield, R. T. (2023). Subspecies-level distribution maps for birds of the Amazon basin and adjacent areas. *Journal of Biogeography*. <https://doi.org/10.1111/jbi.14718>
- Reis, C. A., Dias, C., Araripe, J., Aleixo, A., Anciães, M., Sampaio, I., Schneider, H., & Rêgo, P. S. (2020). Multilocus data of a manakin species reveal cryptic diversification moulded by vicariance. *Zoologica Scripta*, 49(2), 129–144. <https://doi.org/10.1111/zsc.12395>
- Remsen, J. V., & Parker, T. A. (1983). Contribution of river-created habitats to bird species richness in Amazonia. *Biotropica*, 15(3), 223–231. <https://doi.org/10.2307/2387833>
- Ribas, C. C., Aleixo, A., Nogueira, A. C. R., Miyaki, C. Y., & Cracraft, J. (2012). A palaeobiogeographic model for biotic diversification within Amazonia over the past three million years. *Proceedings of the Royal Society B: Biological Sciences*, 279(1729), 681–689. <https://doi.org/10.1098/rspb.2011.1120>
- Ribas, C. C., Fritz, S. C., & Baker, P. A. (2022). The challenges and potential of geogenomics for biogeography and conservation in Amazonia. *Journal of Biogeography*, 49(10), 1839–1847. <https://doi.org/10.1111/jbi.14452>

- Rosser, N., Shirai, L. T., Dasmahapatra, K. K., Mallet, J., & Freitas, A. V. L. (2021). The Amazon River is a suture zone for a polyphyletic group of co-mimetic heliconiine butterflies. *Ecography*, *44*(2), 177–187. <https://doi.org/10.1111/ecog.05282>
- Ruokolainen, K., Moulatlet, G. M., Zuquim, G., Hoorn, C., & Tuomisto, H. (2019). Geologically recent rearrangements in central Amazonian river network and their importance for the riverine barrier hypothesis. *Frontiers of Biogeography*, *11*(3), e45046. <https://doi.org/10.21425/F5FBG45046>
- Salo, J., Kalliola, R., Häkkinen, I., Mäkinen, Y., Niemelä, P., Puhakka, M., & Coley, P. D. (1986). River dynamics and the diversity of Amazon lowland forest. *Nature*, *322*(6076), 254–258. <https://doi.org/10.1038/322254a0>
- Salter, J. F., Brumfield, R. T., & Faircloth, B. C. (2023). An island “endemic” born out of hybridization between introduced lineages. *Molecular Ecology*. <https://doi.org/10.1111/mec.16990>
- Sato, H., Kelley, D. I., Mayor, S. J., Martin Calvo, M., Cowling, S. A., & Prentice, I. C. (2021). Dry corridors opened by fire and low CO₂ in Amazonian rainforest during the Last Glacial Maximum. *Nature Geoscience*, *14*(8), 578–585. <https://doi.org/10.1038/s41561-021-00777-2>
- Sawakuchi, A. O., Schultz, E. D., Pupim, F. D. N., Bertassoli Jr, D. J., Souza, D. F., Cunha, D. F., Mazoca, C. E., Ferreira, M. P., Grohmann, C. H., Wahnfried, I. D., Chiessi, C. M., Cruz, F. W., Almeida, R. P., & Ribas, C. C. (2022). Rainfall and sea level drove the expansion of seasonally flooded habitats and associated bird populations across Amazonia. *Nature Communications*, *13*(1), 4945. <https://doi.org/10.1038/s41467-022-32561-0>
- Scholer, M. N., Kennedy, J. C., Carnes, B. H., & Jankowski, J. E. (2022). Preformative molt, plumage maturation, and age criteria for 7 species of manakins. *The Wilson Journal of Ornithology*, *133*(3), 379–526. <https://doi.org/10.1676/20-00125>
- Schulman, L., Toivonen, T., & Ruokolainen, K. (2007). Analysing botanical collecting effort in Amazonia and correcting for it in species range estimation. *Journal of Biogeography*, *34*(8), 1388–1399. <https://doi.org/10.1111/j.1365-2699.2007.01716.x>
- Sick, H. (1967). Rios e enchentes na Amazônia como obstáculo para a avifauna. In H. Lent (Ed.), *Atas do simpósio sobre a biota Amazônica* (Vol. 5: Zoologia, pp. 495–520). Conselho de Pesquisas Rio de Janeiro.
- Smeds, L., Qvarnström, A., & Ellegren, H. (2016). Direct estimate of the rate of germline mutation in a bird. *Genome Research*, *26*(9), 1211–1218. <https://doi.org/10.1101/gr.204669.116>
- Smith, B. T., McCormack, J. E., Cuervo, A. M., Hickerson, M. J., Aleixo, A., Cadena, C. D., Pérez-Emán, J., Burney, C. W., Xie, X., Harvey, M. G., Faircloth, B. C., Glenn, T. C., Derryberry, E. P., Prejean, J., Fields, S., & Brumfield, R. T. (2014). The drivers of tropical speciation. *Nature*, *515*(7527), 406–409. <https://doi.org/10.1038/nature13687>
- Souza, S. M., Rodrigues, M. T., & Cohn-Haft, M. (2013). Are Amazonian rivers biogeographic barriers for lizards? A study on the geographic variation of the spectacled lizard *Leposoma osvaldoi* Avila-Pires (Squamata, Gymnophthalmidae). *Journal of Herpetology*, *47*(3), 511–519. <https://doi.org/10.1670/12-124>
- Sylvester, Z., Durkin, P., & Covault, J. A. (2019). High curvatures drive river meandering. *Geology*, *47*(3), 263–266. <https://doi.org/10.1130/g45608.1>
- Teófilo, F. H., Schiatti, J., & Anciães, M. (2018). Spatial and environmental correlates of intraspecific morphological variation in three species of passerine birds from the Purus–Madeira interfluvium, Central Amazonia. *Evolutionary Ecology*, *32*(2), 191–214. <https://doi.org/10.1007/s10682-018-9929-4>
- Thom, G., Xue, A. T., Sawakuchi, A. O., Ribas, C. C., Hickerson, M. J., Aleixo, A., & Miyaki, C. (2020). Quaternary climate changes as speciation drivers in the Amazon floodplains. *Science Advances*, *6*(11), eaax4718. <https://doi.org/10.1126/sciadv.aax4718>
- Tsai, W. L. E., Schedl, M. E., Maley, J. M., & McCormack, J. E. (2020). More than skin and bones: comparing extraction methods and alternative sources of DNA from avian museum specimens. *Molecular Ecology Resources*, *20*(5), 1220–1227. <https://doi.org/10.1111/1755-0998.13077>
- Valencia, R., Balslev, H., & Paz Y Miño C, G. (1994). High tree alpha-diversity in Amazonian Ecuador. *Biodiversity and Conservation*, *3*(1), 21–28. <https://doi.org/10.1007/bf00115330>
- Van der Auwera, G. A., & O’Connor, B. D. (2020). *Genomics in the cloud: Using Docker, GATK, and WDL in Terra*. O’Reilly Media.
- Wallace, A. R. (1852). On the monkeys of the Amazon. *Proceedings of the Zoological Society of London*, *20*, 107–110.
- Weir, J. T., Faccio, M. S., Pulido-Santacruz, P., Barrera-Guzmán, A. O., & Aleixo, A. (2015). Hybridization in headwater regions, and the role of rivers as drivers of speciation in Amazonian birds. *Evolution*, *69*(7), 1823–1834. <https://doi.org/10.1111/evo.12696>
- Zhang, Z. -Y., Zheng, X. -M., & Ge, S. (2007). Population genetic structure of *Vitex negundo* (Verbenaceae) in Three-Gorge Area of the Yangtze River: the riverine barrier to seed dispersal in plants. *Biochemical Systematics and Ecology*, *35*(8), 506–516. <https://doi.org/10.1016/j.bse.2007.01.014>